NASA TECHNICAL MEMORANDUM

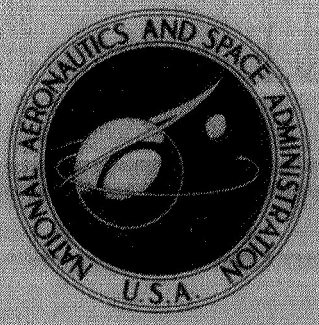

NASA TM X-2150

NASA TM X-2150

MODIFICATIONS OF THE CYGRO-2 COMPUTER PROGRAM

by Ivan B. Fiero

Lewis Research Center
Cleveland, Ohio 44135

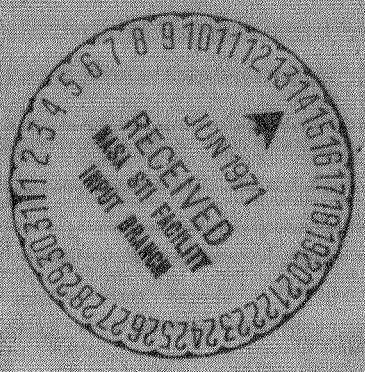

NATIONAL AERONAUTICS AND SPACE ADMINISTRATION • WASHINGTON, D. C. • MAY 1971

1. Report No.	2. Government Accession No.	3. Recipient's Catalog No.
NASA TM X-2150		

4. Title and Subtitle	5. Report Date
MODIFICATIONS OF THE CYGRO-2 COMPUTER PROGRAM	May 1971
	6. Performing Organization Code

7. Author(s)	8. Performing Organization Report No.
Ivan B. Fiero	E-5905
	10. Work Unit No.
9. Performing Organization Name and Address	120-27
Lewis Research Center National Aeronautics and Space Administration Cleveland, Ohio 44135	11. Contract or Grant No.
	13. Type of Report and Period Covered
12. Sponsoring Agency Name and Address	Technical Memorandum
National Aeronautics and Space Administration Washington, D.C. 20546	14. Sponsoring Agency Code

15. Supplementary Notes

16. Abstract

Modifications made at Lewis to the CYGRO-2 computer program are presented. The CYGRO-2 program is a Westinghouse-Bettis-developed program for the mechanical analysis of irradiated, cylindrical geometry, nuclear reactor fuel pins subjected to fuel swelling due to fission products. The modified program is compatible with the Lewis IBM 7094 computer. Results of the modifications are shorter computer times and improved convergence. A sample problem for a uranium mononitride fuel pin is included, with detailed discussion of input data and the difficulties encountered therewith. Computer problems encountered in using the program are detailed both in the discussion of the modification and in the discussion of the sample problem.

17. Key Words (Suggested by Author(s))	18. Distribution Statement
Fuel swelling Fuel-pin swelling Fuel-pin deformation Irradiation swelling	Unclassified - unlimited

19. Security Classif. (of this report)	20. Security Classif. (of this page)	21. No. of Pages	22. Price*
Unclassified	Unclassified	51	$3.00

*For sale by the National Technical Information Service, Springfield, Virginia 22151

CONTENTS

MODIFICATIONS OF THE CYGRO-2 COMPUTER PROGRAM

by Ivan B. Fiero

Lewis Research Center

SUMMARY

The CYGRO-2 computer program is a potentially useful tool in analytically predicting fuel-element swelling for the cylindrical geometry, nuclear reactor fuel pins. The program takes into account many facets of the behavior of irradiated fuel pins. These include fuel swelling, fuel-clad interaction, thermal gradients, and plastic and creep behavior. However, the program as it existed was not compatible with the Lewis IBM 7094 computer. It had inherent problems associated with application to this computer and associated with techniques used to solve equations within the program.

The program was modified such that it would be compatible. However, many difficulties were encountered while using the program. Termination before completion often occurred in conjunction with various sorts of computer diagnostics. These computer diagnostics, once loading was achieved, consisted mainly of overflows, underflows, divide by zero, and too large exponents. Also, the program often utilized very small time steps. Several modifications were made to the program to alleviate these difficulties. These modifications can be summarized as three main categories: (1) modifications in the techniques of solving certain simultaneous equations and methods of averaging variables for a given time step, (2) optional changes such as printout options to aid in debugging and some additional input and output which are useful to the program user, and (3) changes in FORTRAN form and range of subscripts and general shortening for application to the Lewis computer.

The resulting modifications not only caused the program to run as was primarily desired, but resulted in decreased computation times and improved convergence. The improved computation times were very significant in some instances.

A sample problem of a uranium mononitride fuel pin has been included to show the changes that have been made to the input data deck and the printout received from the modified CYGRO-2. Changes to the data deck include modification of the initial comments cards and an inclusion of two additional pieces of data. The printout format was changed slightly and a few more variables were added to the print list. Various problems associated with the input data are also discussed.

INTRODUCTION

The CYGRO-2 computer program (ref. 1) is a potentially useful tool in analytically predicting fuel-element swelling and growths for the cylindrical geometry, nuclear reactor fuel pins. It was written by Friedrich and Guilinger of Westinghouse-Bettis as a development from a group of individual computer programs (such as FIGRO, CYGRO, and CYGRO-1; refs. 2 to 6) to calculate the effect of swelling fuel, fuel-clad interactions, and pin design. Basically, the program is based on a two-material zone (fuel zone and clad zone), cylindrical geometry fuel pin constrained by a plane strain assumption. This assumption best applies to long cylinders, where the effect of end constraints and multiple pellets are neglected.

The fuel may or may not contain a central void or plug and there may be an initial gap between fuel and clad. The program utilizes viscoelastic behavior determined by both a normal creep rate associated with second-stage creep and an accelerated creep which corresponds to plastic flow. Usual constraints of equilibrium and compatibility are assumed. Mechanical loads originate from thermal expansions, gas pressures, and irradiation swelling. Irradiation swelling depends on (1) solid fission products generated and deposited within the fuel and fragmented into the clad and (2) gaseous fission products. All the swelling associated with gaseous fission products is assumed to be the result of coalescing into a set number of inter- and intragranular bubbles. Gas bubble growth depends on an equilibrium between bubble pressure, surface tension, creep forces adjacent to the bubble, and the spherical stress in the surrounding material. Stress in the surrounding material is dependent on the forces arising from thermal gradients and fuel-clad interactions. Fuel cracking and fuel-clad interface slip are not considered in this version of CYGRO, although they are included in a later version (ref. 7).

The program achieves solution by a finite difference formulation. Due to axial symmetry, the only geometric variable is radius, which is divided into thin cylinders or rings. Also, the program is quasi-transient, which means small time increments or steps are utilized, during which rate variables are assumed to be constant.

The advantage of such a complicated program as CYGRO-2 is that it takes into account much of the behavior that is known to take place within irradiated fuel pins. For example, it includes thermal expansions, creep and plastic flow, generation of fission products requiring more volume than the initial material occupied, releasing of gas into plenums or voids, and sintering and hot pressing behavior. However, there are certain disadvantages in that (1) input is lengthy and complex, (2) some input is difficult to evaluate (such as gas gap pressure, which can be strongly dependent on fuel swelling), (3) the complex interrelations of parameters involved makes it difficult to predict the effect of changes in certain parameters in advance, and (4) such a complex program

requires considerable computer time. A direct disadvantage of the complex input is that, in order to generate proper data, knowledge of fuel behavior is required, a priori. For example, the solid volume expansion of bare fuel must be known and the number of bubbles as a function of temperature must be known. These are only roughly or empirically known from previous fuel-pin tests, or are only known for some particular final burnup at the present stage of understanding of swelling of nuclear fuels. Hence, even though the program is versatile it is left to the discretion of the user to model the fuel pin adequately.

Several difficulties were encountered with the use of CYGRO-2 on the Lewis IBM 7094 computer. These consisted at the outset mostly of underflows, overflows, divide by zero, too large exponents, and basic core storage problems. In addition, the program was utilizing very small time steps, resulting in large running times for small problem times. These operating difficulties occurred from time to time and were dependent on and sensitive to fuel-pin geometry and power history.

Resulting modifications made to the CYGRO-2 computer program were in three main categories: (1) modifications in the techniques of solving certain simultaneous equations and methods of averaging variables for a given time step; (2) optional changes, such as printout options, to aid in debugging and some additional input and output; and (3) initial changes in FORTRAN form and range of subscripts and, finally, general shortening for application to the Lewis computer. These modifications not only caused the program to run as was primarily desired, but also resulted in decreased computation times. The improved computation times were very significant in some instances. Another advantage of some of the modifications was an improved accuracy.

This report summarizes the modifications made to CYGRO-2 and presents a sample problem which was solved using the modified version of CYGRO-2. No attempt is made to discuss the modifications on a FORTRAN statement basis, but rather in general terms, with an attempt to be as consistent as possible with symbols and terminology of reference 1. It is assumed herein that the reader is familiar with reference 1.

The modifications made to the program are presented first. Then a detailed sample problem for a uranium mononitride fuel pin follows, with a discussion of the input data cards. Included under the data card description is a discussion of difficulties with the input data in relation to results obtained on the computer.

MODIFICATIONS

Calculation Technique

Conductivity as a function of porosity. - The program requires conductivity for the fuel and clad in order to determine temperature distributions within the fuel pin. The conductivity can be expressed as a function of the porosity or density of the material by appropriate constants, as discussed in reference 1.

An error can occur, however, if only a fraction of the solid material, rather than 100 percent, is associated with the bubbles. If this is done, the apparent density within the program is not the true density and the resulting conductivity is incorrect. This is due to the particular parameter being utilized to make the density corrections. In fact, the solid volume fraction unaccounted for, or not utilized around any type of bubble, becomes part of the porosity. The equations were modified slightly so that the gas bubble volume is summed over all bubble types. The sum is divided by the total gas-plus-solid volume to obtain a density ratio V_{gh}/V. This is the ratio described in reference 1. One of the FORTRAN common blocks had to be moved into the subroutine to make the correct variables common for the modification. These density corrections are performed in subroutine SEGT.

Variable gas generation rate in fuel rings. - Required gas bubble information for the fuel pin includes the moles of initial gas, fission gas generation rate coefficients, diffusion or leakage coefficients, volumes of the bubbles and solid material volumes associated with the bubbles for each type of bubble, and the number of bubbles. The only variables dependent on both the material, fuel or clad, and the individual rings are the moles of initial gas, the volumes of gas bubbles, and the number of bubbles. The others are only material dependent. However, this specified information is for each bubble type and the dependency on rings and/or material can be specified for each bubble type.

In some instances, it was found that it would be advantageous to have the fission gas generation coefficient as a function of the rings. Consequently, the subscript was changed from a dual subscript on the gas bubble types and material to a subscript set on the gas bubble types and rings Both subscript variable FORTRAN name and subscript range dimension required changing. In this way a radially dependent gas generation can be utilized, if desired, which would reflect a radial flux variation. These changes were made in the subroutine dealing with gas bubble calculations, subroutine SGAS.

Gas bubble equilibrium. - Bubble equilibrium and bubble expansion or contraction are determined in the subroutine SGAS. The gas bubble is acted upon by several forces:

(1) Gas pressure due to initial gas present (fabrication porosity) and to fission gases which accumulate as bubbles. (Buildup of gas pressure tends to expand the bubble and cause the fuel growth phenomenon.)

(2) Surface tension of the gas bubble - solid interface, which tends to reduce or restrict bubble growth. (This is the sintering force (ref. 1) which, under application of no other force, tends to sinter the material from its fabricated porosity.)

(3) Macroscopic stress in the surrounding material, which acts as a hydrostatic pressure and can cause the hot pressing of partially dense material (ref. 1).

(4) The equivalent creep stress set up in the material due to a change in bubble size (creep rate is directly related to the bubble growth rate), which also acts to restrict bubble growth.

A summation of these forces must be zero at the bubble-solid interface for the bubble to be in equilibrium.

The CYGRO-2 program, it was discovered, spent a major portion of the computer time doing iterations to converge on an equilibrium (balance of forces) situation. The technique of convergence consists of summation of forces against bubble growth rate until the summation is zero. It was not unusual for the program to take 400 to 500 iterations through a long series of equations to converge on a solution. This part of the program was rewritten to change the method of convergence. A typical case now converges in about six to eight iterations. This modification reduced overall run time by a factor of 4 or 5 for some problems.

Previously, if an iteration resulted in nonconvergence in equilibrium, the next iteration merely adjusted the bubble growth rate by some very small amount and recycled through the calculations. Now, the new bubble growth rate, after two iterations over a much wider range of bubble growth rate, is modified according to slope and/or sign of the resultant force (or pressure) around the bubble (modified method of succession approximations, ref. 8). This is a rather complicated set of equations because the curves (bubble growth rate against summation of pressure forces at bubble-solid interface) describing the iteration scheme are not well behaved. In general, they are somewhat hyperbolic and can have blips or small changes in slope along the asymptotic portions. In addition, three modes of creep or plastic flow can cause discontinuities. These three modes are associated with the physical problem in that the material surrounding the bubble may be only in creep flow, in both creep and plastic flow, or entirely in plastic flow.

It was also found that occasionally the iteration scheme could not find an equilibrium condition for the bubble. An example of this is when the hyperbolic-shaped curve does not have a solution but becomes asymptotic to the axis representing a solution, or contains a small blip so that the curve appears to diverge from any solution. Previously, when this occurred, the answer closest to the equilibrium condition was used. It was

found that utilizing this answer results in an instability in the stress calculation for a given fuel node and also results in abnormal fuel swelling for that fuel node. These results, of course, affect the calculations in the time steps following. This particular problem would also exist with the new accelerated convergence method unless the program were modified such that the time step could be decreased. It was found that a smaller time step would always cause a shift in the curve, resulting in a solution.

Consequently, the subroutine was modified with a routine that decreased the time step to a value such that bubble equilibrium could be achieved. The controlling variable in the routine is called JERK. Essentially, what happens is that when such a condition of nonequilibrium occurs, this variable (JERK) is set equal to the larger of two values, either 2 or a ratio proportional to how far from equilibrium the problem is. The program is then forced to exit from the subroutine SGAS for the particular node for which it was calculating gas bubble equilibrium. All the remaining nodes are cycled through to obtain the largest value of JERK. Then the program returns to subroutine STIM where the time step is divided by JERK and the calculations begin again. The number of times this nonequilibrium occurs is printed out at the end of the problem and has been as high as 25 in some of the problems run thus far. This is out of a thousand or more time steps.

The routine was also later remodified to decrease the time step when two other problems arise. On occasion, the method of convergence set up would not be able to find a solution in a reasonable number of iterations. One occasion was when a small blip would occur. It is nearly impossible to detect these blips in all possible cases; and after several debugs to correct this situation, it was decided that a unique set of circumstances could, on any new problem, result in not converging on a solution. Consequently, after an unreasonable number of iterations (100 was deemed unreasonable) the program utilizes the JERK variable to reduce the time step.

Secondly, there are three possible modes of creep and plastic behavior around the bubble, each of which greatly affects the shape of the curve. These are physically related to conditions where the material surrounding the bubble is in creep only, the material is partially in creep and partially in plastic flow, or the material is entirely in plastic flow. The program would often cycle between modes, looking for the correct solution. Occasionally, the cycling was excessive because the modes exhibited a discontinuous behavior between modes; that is, one mode approached $+\infty$, whereas the next mode approached $-\infty$. Whenever the program cycled between modes an excessive number of times, the time step was also decreased by the variable JERK. In this case, since the usual number of times was only once or twice, the program was set to utilize JERK if it cycled at least 25 times. Satisfactory results have been obtained for both of these situations, with no significant increase in the number of times JERK has been utilized. Apparently, this problem occurs only rarely.

These modifications to the subroutine SGAS have had the beneficial effect of both greatly decreasing computer time and improving accuracy.

Fuel-clad gap closure. - Contact between the fuel and clad occurs because the radial growth of the fuel overtakes that of the clad. In the program the growth during a given time step may exceed that of the clad and give a sudden interference fit, providing the interference force does not exceed a specified amount. This interference is corrected in the next time step. However, the initial interference is frequently so great that it causes irregularity in the stresses and strains of the fuel and clad. Rates of stress and strain can be affected enough that, once contact occurs in this manner, the program calculates negative contact forces in the following time step. This period during the history of the fuel pin causes special problems and in the CYGRO-2 program (ref. 1) is called the "twilight" period.

Now, rather than utilize the full time step, which would cause an interference fit, the time step is proportionally reduced to cause gradual contact. A check is made to see if an interference is going to occur. If so, the time step is reduced an amount proportional to the ratio of the actual gap to the actual gap plus interference. An additional arbitrary multiplier of 0.9 is used so that the contact is approached smoothly. This results in a few more iterations initially, but because of the smoother action resulting from this method of contact, the overall number of iterations is generally reduced. And there are no irregularities in the stresses and strains during this "twilight" period.

Smallest time increment and gap closure criterion. - The CYGRO-2 computer program utilizes a very small number (10^{-20}) to represent limitations on two parameters. It is defined by an arithmetic statement in the program and is alterable only by changing the FORTRAN. It is used (1) for the convergence criterion for the fuel-clad contact (the point at which the radii are set equal), and (2) as the smallest possible time step allowed (defined as TINY). The time step can decrease due to a number of factors: rates of stress or strain may be too large; fuel-clad contact interference may reduce the time step; or problems may arise with fission gas bubble equilibrium calculations, as previously discussed.

It was felt that 10^{-20} was too small for these purposes for two reasons. First, as a convergence criterion for the fuel-clad contact, it would be significant enough to use something much larger, say 10^{-7}. Secondly, this small time step was not utilized by the program unless there were other problems which indirectly required a small time step and needed corrective action separately. When the small time step (TINY) was used, none of the variables appeared to change. For example, it made no difference in the values of the variables whether 10^{-7} was used or 10^{-20}. It simply took slightly longer to work down to the smaller number. Consequently, it was felt that the smaller number served no real useful purpose and it was changed to 10^{-7}. This means that, when the gap is closed to within 10^{-4} mils (2.54×10^{-7} cm), the radii are set equal.

These changes are required to the subroutine STIM and also in the main program to a related variable called STINY.

Another problem which has occurred, and is complicated by the previously discussed modifications to subroutine SGAS, is that the program automatically bypasses the gas equilibrium calculations when this small time step (TINY) is used. It may be wise to further modify the program such that it cycles through the gas calculations even when the small time step is used. This is especially true during sintering when the bubble collapse results in the gas calculations being the governing factor for decreasing the time step. It is obvious that when the subroutine SGAS is responsible for the decreased time step, it should not in turn be bypassed. This bypassing of subroutine SGAS is also the reason that sometimes none of the variables appear to be changing when TINY is used. A slight modification to the subroutine SGAS would cause the calculations to always be made. However, this change has not as yet been incorporated into the modified CYGRO-2.

Smaller initial time step. - The initial time step, after a new time card was read, was originally chosen as 1/100 of the time interval between two consecutive time cards. If the problem required a lesser time, and it usually did, it could obtain it in several iterations by the routine previously discussed. This was modified to use the smaller of either 1/100 of the time interval or 0.1 hour for the initial time step. This helps to reduce the number of iterations when there is a large interval of time between two consecutive time cards. It does not unnecessarily restrict the time step because the following time step is always of a magnitude commensurate with the new defined rates of stress and strain.

It is of interest to note that this change primarily originated from problems previously encountered in gas equilibrium calculations which were subsequently alleviated by the modifications made to subroutine SGAS. However, this change was retained because of potential savings in computer time.

Self-initiated time step reduction. - The program often requires a reduction in the time step as previously discussed, and can require several iterations to find a useable one. Consequently, a technique was employed by which the convergence to a useable time step is greatly accelerated. This technique is a greatly modified method of successive approximations, and occurs in subroutine STIM. The procedure is as follows: The time increment or time step called DTIME is the actual time step being used. All the appropriate calculations are made using this time step, including the rates of stress and strain. The inputed allowable stress and strain changes are then divided by these stress and strain rates, respectively, to obtain a new time step called DELTA. This DELTA represents the time step which could be used in order for the stress and strain changes to just equal the allowable. If the DTIME used is greater than DELTA, which implies that the stress and strain changes would have exceeded the allowable, DTIME is

set equal to DELTA and all the calculations are redone. Both the time step DTIME and the required time step DELTA are stored for any two consecutive iterations. If DTIME is less than DELTA, the stress and strain changes will be less than the allowable. In this case DTIME is kept as a reasonable time step and DELTA is used for the next time step. It is important to note that the DELTA does not remain constant, which is the reason that more than two iterations are required. The DELTA is dependent upon DTIME in a nonlinear fashion. However, the optimum time step is one in which the stress or strain change just equals the allowable change. Therefore, the optimum DTIME is one which is just equal to DELTA, and this is the basis for which a new estimated time step is determined. In other words, when two consecutive DTIME's and the resulting DELTA's (since DELTA is actually indirectly dependent on DTIME) are known, a slope can be determined and extrapolated to a condition where these parameters are equal. This technique has greatly reduced the number of iterations and reduced computer time.

Allowable stress and strain rates. - The stress and strain rate during a given time step must be less than, or equal to, that value which, if multiplied by the time step, would result in an incremental change equal to the allowable values specified in the program input data. For example, it may be decided that it would be unreasonable to allow a step change in the stress of more than 1000 psi (689 N/cm^2) or a strain change of more than 10^{-3} inch per inch (10^{-3} cm/cm).

Furthermore, the stress and strain changes in the CYGRO-2 computer program during a given time step are each composed of two parts. These two parts, as defined in reference 3, can be expressed as parts of the total stress and strain change as

$$\Delta S = \Delta S_i + \dot{S}\,\Delta t$$

$$\Delta \epsilon = \Delta \epsilon_i + \dot{\epsilon}\,\Delta t$$

respectively, for the stress change and strain change; and where ΔS_i and $\Delta \epsilon_i$ are stress and strain changes assumed to take place at the beginning of the time step (ref. 3, p. 23), and the stress and strain changes $\dot{S}\,\Delta t$ and $\dot{\epsilon}\,\Delta t$ are those taking place during the time step. (All symbols are defined in appendix A.)

Originally, the program compared only the second terms, $\dot{S}\,\Delta t$ and $\dot{\epsilon}\,\Delta t$, with the allowable stress and strain changes. However, a debug of the program revealed that the second terms are often equal in magnitude but sometimes opposite in sign to the first terms. Because of this, the time step can be unnecessarily restricted in some cases or allow too large a total change ΔS or $\Delta \epsilon$ in other cases. Consequently, the program was modified to compare the total stress and strain change with the allowable value. This is accomplished in subroutine STIM.

Special restrictions on change in equivalent stress. - The subroutine STIM contains certain sign restrictions on the change in equivalent stress. For example, if the projected equivalent stress is negative, with certain exceptions, the time step may be reduced. The technique by which the time step is reduced can be relatively unstable when the equivalent stress is near zero; such as at the beginning of the problem or when a particular node (or ring) is near zero equivalent stress. It was possible to reduce the time step by orders of magnitude under such conditions. This was corrected by letting the variable containing the initial equivalent stress be the greater of either its natural calculated value or 500 psi (345 N/cm^2). Consequently, the time step is not reduced when the change in equivalent stress and the equivalent stress are small. However, this procedure still may result in an unnaturally small time step when by chance the variable is negative but slightly greater than 500 psi (345 N/cm^2) in magnitude. It is not known just how often this may occur, and further modification may be required.

Time step at closure of time interval between time cards. - As the problem time approaches that of the value on the input time card, a check is made to see if the remaining time is less than the smallest allowed (TINY). If so, the time step DTIME is set equal to TINY and is used for the remainder of the calculations. Consequently, the final time can exceed the time-card time by some small amount. Since the value of the smallest time step allowed has been increased, as previously discussed, this section was slightly modified to use, in this case, either TINY or the remaining time, whichever is smaller. This modification also occurs in subroutine STIM.

Calculation of strain rates. - The total generalized strain ϵ_g is obtained by integration of the generalized strain rate $\dot{\epsilon}_g$. The value of $\dot{\epsilon}_g$ is approximated from the initial values of the independent variables and from the rates of change of these variables. The calculated strain rate is then assumed to be constant during the time step. All the calculations used in determining this $\dot{\epsilon}_g$ are in subroutine SEGT. Originally, subroutine SEGT contained two separate and independent methods of obtaining $\dot{\epsilon}_g$. Only one ever appeared to be utilized. A logic statement always routed the calculations to only one of the methods. Each of these methods and the resulting modification to the program are discussed.

The first method utilized the technique outlined in reference 1. The expression for strain rate (ref. 1) is

$$\dot{\epsilon}_g = A_{gt} + A_{gg}\dot{S}_g$$

where

$$A_{gt} = \frac{f_{eg}(\epsilon_l, S_g)}{1 - \frac{\partial f_{eg}}{\partial \epsilon_l} C_{lg} \Delta t}$$

$$A_{gg} = \frac{\frac{\partial f_{eg}}{\partial S_g} \Delta t}{1 - \frac{\partial f_{eg}}{\partial \epsilon_l} C_{lg} \Delta t}$$

Derivatives are formulated into a finite difference form. The derivative $\partial f_{eg}/\partial S_g$ is evaluated by calculating the generalized strain rate f_{eg} associated with two different stress levels and keeping the equivalent plastic strain ϵ_l constant. Because this strain defines the intersection of the curves for creep and for plastic flow (fig. 1(b)), this intersection also remains constant. The two stress levels are determined by taking equal stress increments of $\pm\Delta S$ on either side of the equivalent stress S_g, as shown in figure 1. The magnitude of ΔS is the same as the maximum allowable stress change specified in the program input. The derivative is then formed or approximated by the change in f_{eg} with respect to the overall change in S_g. The derivative $\partial f_{eg}/\partial \epsilon_l$ is evaluated by keeping S_g constant and calculating the strain rate associated with a new equivalent strain ϵ_l found by adding onto the current ϵ_l a $\Delta\epsilon$, as shown in figure 2. This effectively translates the plastic creep line to a higher stress on the creep curve, where the new intersection between regular creep and plastic creep is at the plastic stress corresponding to a plastic strain of $\epsilon_l + \Delta\epsilon$. The $\Delta\epsilon$ is the maximum allowable strain change specified in the program input. As shown in figure 2(b), the change in f_{eg} is zero unless the plastic flow line is involved. The value of f_{eg} in the equation is determined from current values of ϵ_l and S_g at the beginning of the time step. Both of the derivatives in the equations have been approximated and a value for $\dot{\epsilon}_g$ can be calculated.

It was found upon initial application of CYGRO-2 that this method could result in erratic stresses. Not only did the stresses change erratically with respect to time, but also with respect to radius. This method resulted in several mathematical problems. First of all, the derivative $\partial f_{eg}/\partial \epsilon_l$ must be small or, when the quantity $1 - (\partial f_{eg}/\partial \epsilon_l) C_{lg} \Delta t$ is evaluated, the result is a negative number. Consequently, the strain rate $\dot{\epsilon}_g$ is projected as negative, which is not physically possible. Large values for the derivatives are possible when the equivalent stress is high enough that increasing

the strain an increment $\Delta\epsilon$ (at constant S_g) moves the stress-strain loci from a region of plastic flow (or creep) into a region of regular creep. A second problem, and one which occurs more often than the previous, is that the creep rate associated with $S_g + \Delta S$ may be many orders of magnitude greater than that of S_g. This becomes more obvious when S_g is very close to yield point. Then, when ΔS is added, the stress is above the plastic stress. Combining this with the concept that the plastic flow or creep curve is nearly vertical ($\log \dot{\epsilon}_g$ with respect to $\log S_g$), $\dot{\epsilon}_g$ must be very large at $S_g + \Delta S$. This could lead to an unstable situation. For example, if the strain rates in two adjacent nodes are considerably different, unstable stress distributions could result. These problems could be alleviated somewhat by making the required ΔS and $\Delta\epsilon$ very small. This procedure, however, would result in much larger computer times. Consequently, the subroutine SEGT was slightly modified so that only the second method would be utilized. This second method gave much smoother stress distributions.

The second method of calculating the generalized strain rate $\dot{\epsilon}_g$ utilizes the amount of strain which would occur if the strain rate existing at the beginning of the time step were applied throughout the time step. Here the basic derivatives being evaluated are slightly different. It is assumed that the equivalence between the product $(\partial\dot{\epsilon}_g/\partial S_g)\Delta t\dot{S}_g$ and $(\partial\epsilon_g/\partial S_g)\dot{S}_g$ can be utilized so that the derivative $\partial\epsilon_g/\partial S_g$ can be evaluated rather than $\partial\dot{\epsilon}_g/\partial S_g$. Initially, all that is known at the beginning of the time step is the equivalent strain ϵ_l (or ϵ_g, depending on whether it is a cyclic problem (ref. 1)), the plastic stress of this particular strain, the equivalent stress S_g, and the strain rates associated with both the equivalent stress and the plastic stress. It is initially assumed that the strain rate f_{eg} occurring at the beginning of the time step occurs throughout the time step. The new value of the strain at the end of the time step is determined and the required stress to maintain this constant strain rate is solved for. This essentially moves the intersection on the creep - plastic flow ($\log S_g$ - $\log \dot{\epsilon}_g$) curve to a higher stress, as shown in figure 3. The new required stress is that found on the new creep - plastic flow curve (fig. 3(b)), keeping $\dot{\epsilon}_g$ constant. The intersection is found from the plastic stress-strain characteristic diagram. These values of S_g and ϵ_g are defined as the upper limits, with lower limits of the differences yet to be defined in order to evaluate the derivative $\partial\epsilon_g/\partial S_g$. Now a strain rate must be assumed which will result in the lower limits. A higher rate can be assumed for the purpose of finding $\partial\epsilon_g/\partial S_g$; however, it is more probable that a lower rate, resulting in lower strain, is more accurate because of such factors as stress relaxation. CYGRO-2 uses a lower strain rate. The lower strain rate is assumed to be the arithmetic average of the initial strain rate and the final strain rate at the end of the time step. This new lower strain rate, and consequently, lower strain, defines a new $\log S_g$ - $\log \dot{\epsilon}_g$ intersection; and consequently, there is a definite stress required to obtain this strain rate. The derivative can then be formed. If the difference between the upper and lower strains $\epsilon_{g,up} - \epsilon_{g,low}$

is more than the $\Delta\epsilon$ requirement specified in the input data, the strain $\epsilon_{g,\,low}$ is set equal to the upper strain minus $\Delta\epsilon$. The appropriate strain rate is determined which will satisfy this new lower strain. If the stress difference $S_{g,\,up} - S_{g,\,low}$ violates ΔS requirement specified in the input data, the new lower strain is modified by another factor to move the lower strain nearer to the upper strain. After both of these requirements are met, the derivative $\partial\epsilon_g/\partial S_g$ is formed. By using the difference between these upper and lower limits of strain, the equivalence previously discussed is satisfied; that is,

$$\frac{\partial\dot{\epsilon}_g}{\partial S_g}\Delta t = \frac{\dot{\epsilon}_{g,\,up} - \dot{\epsilon}_{g,\,low}}{S_{g,\,up} - S_{g,\,low}}\Delta t = \frac{\dot{\epsilon}_{g,\,up}\,\Delta t - \dot{\epsilon}_{g,\,low}\,\Delta t}{S_{g,\,up} - S_{g,\,low}} = \frac{\epsilon_{g,\,up} - \epsilon_{g,\,low}}{S_{g,\,up} - S_{g,\,low}} = \frac{\partial\epsilon_g}{\partial S_g}$$

where the difference between the upper and lower strain limits is used, rather than a difference from the strain at the beginning of the time step. This second method uses essentially the equation

$$\dot{\epsilon}_g = A_{gt} + A_{gg}\dot{S}_g$$

where

$$A_{gt} = \dot{\epsilon}_g\Big|_{S_g}$$

$$A_{gg} = \frac{\partial\epsilon_g}{\partial S_g}$$

and where $\partial\epsilon_g/\partial S_g$ is evaluated as previously described, and A_{gt} is evaluated by holding S_g constant and determining what the effective strain rate must be. This is not simply a constant creep rate, especially if the stress is in the plastic flow region. (This is because of the shifting of the intersection on the $\log S_g$ - $\log \dot{\epsilon}_g$ curve.) Once the strain is determined for constant S_g, the strain rate may be determined. The strain is determined by utilizing the preceding derivative for A_{gg}. The strain is extrapolated backwards to S_g from the upper stress using the slope. The strain rate is then determined from this strain.

It was found that this procedure always underestimates the amount of strain rate $\dot{\epsilon}_g$ and, in fact, sometimes extrapolates to negative strain rates. This appears in the CYGRO-2 output as zero strain rate because only strains greater than, or equal to,

zero are allowed. A check revealed that this can be very seriously in error because the curve is assumed to be linear for extrapolation. However, an evaluation shows it to be extremely nonlinear; consequently, when the extrapolation occurs over large stress changes, a large error occurs. This is shown in the following sketch, where the solid line represents the extrapolation and the large-dashed line represents the true behavior:

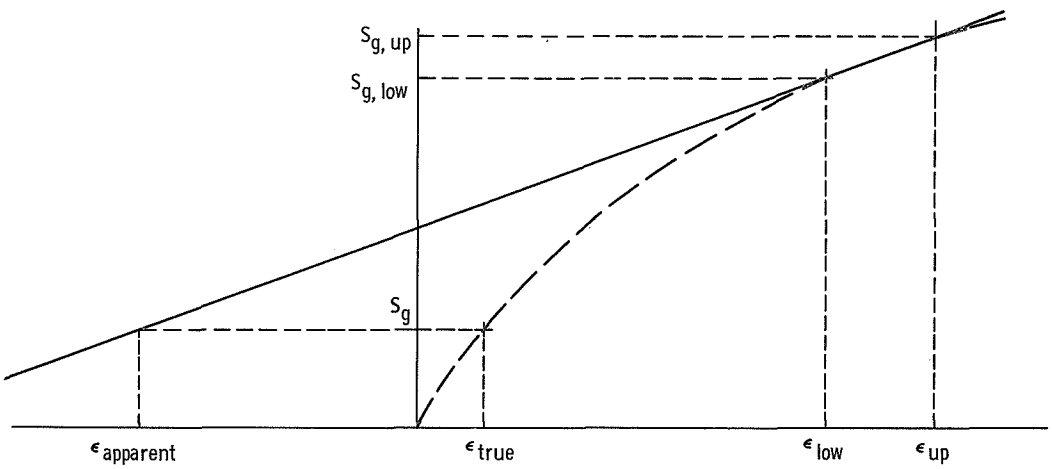

Therefore, the subroutine was modified to obtain more accurate estimates for the strain rates. It was felt that the easiest way to attack this problem would be to modify the second method, since the only changes required would be to use an alternate method of determining the strain rate at constant S_g. The first method was retained within the program although it is not utilized.

The strain rate is again evaluated from the equation

$$\dot{\epsilon}_g = \dot{\epsilon}_g\Big|_{S_g} + \frac{\partial \epsilon_g}{\partial S_g}\dot{S}_g$$

where the value of the strain rate assuming constant stress can be obtained easily from the creep curves. An examination of the following sketch shows how this can be done by an iteration technique:

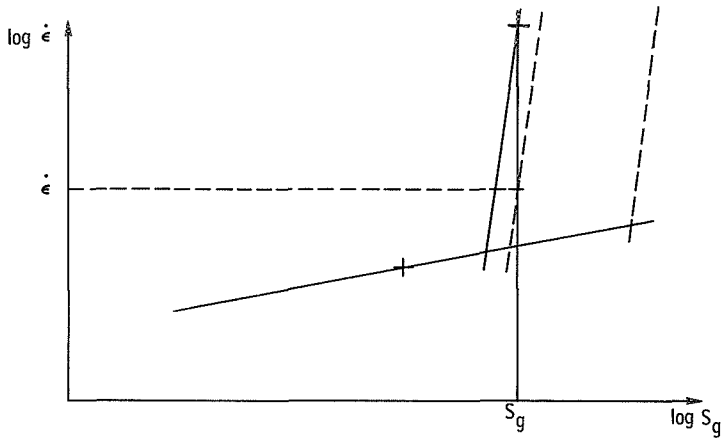

It must be remembered that the intersection between the regular creep line and the accelerated creep or plastic flow line is affected by the creep assumed to have taken place during the time step. Consequently, if the stress S_g is above the plastic stress, an iteration scheme is required; if below, no iteration is required. The object is to find the value of strain rate (indicated by $\dot{\epsilon}$) while keeping S_g constant, which satisfies both the constant stress and change in position of the intersection due to the change in strain. It is obvious that only one such solution exists. An iteration scheme finds this solution in just a few iterations. A value for the first term in the strain rate equation is then known.

Next, the value of the derivative $\partial\epsilon_g/\partial S_g$ must be found. This procedure was left nearly identical to the original CYGRO-2, with the exception that the lower value of the strain rate becomes that which was just solved for. Consequently, this slope is based upon strain rates which are closer to those just deviating from the condition of constant stress S_g.

With this scheme there are no resulting zero strain rates with finite stresses, and the slight increase in iterations in this small area adds no significant amount of computer time. It might be mentioned that previous to this change a particular situation existed such that the stress in one of the nodes of a sample problem was increasing but the creep rate was zero. After a few time steps the stress became so large an overflow occurred.

Optional Modifications

The CYGRO-2 program was further modified to give additional calculations and additional printout of the calculated parameters than what was done in its original form.

It was also modified slightly to give a different comment card format for the data deck and a slightly different printout format.

Input titles for the data deck were altered. Any number of comment cards can be read in and printed previous to the data. The number of title cards is controlled by the first two columns on each card. As long as the space is left blank, continual reading of additional comments cards occurs. The last card then contains a number and the next card must be a regular data card (card 900). This allows a very descriptive set of comments so that different problems being run are easily distinguishable.

The printed output which was divided into groups was modified in two ways. The write format was changed so that the data are spread out more; in other words, simply more space between numbers. Secondly, more frequent printout is obtained. Originally, a printout of groups 3 to 7 (ref. 1) occurred at each time card. Now a counter called MMM controls additional printout between time cards of group 4, and a counter called NNN controls the printout between time cards of groups 4 to 7. These are essentially print frequency counters. They are specified on one of the input cards: card 907, items 7 and 8. For example, if MMM equals 5 and NNN equals 10, every fifth time step, regardless of elapsed time, would result in group 4 being printed and every 10th time step, groups 4 to 7. The program still prints the entire group (3 to 7) when the elapsed time equals that specified on the time cards. The additional printout allows the calculations and progress to be followed much better. Group 4 contains time, critical dimensions, maximum stresses and strains, and contact forces. Groups 5 to 7 include individual ring data on temperatures, radii, stress and strains, and volume growths, and bubble information.

One additional printout of all data occurs at the point in time where the fuel and clad have just contacted. These data provide useful information on free fuel growth and exact contact time.

An additional output parameter was included in the group 4 printout which indicates whether plastic flow (accelerated creep) or regular creep has taken place in each of the rings of fuel or clad during the time step. The plastic flow index is zero for creep, a normal condition until the equivalent stress exceeds the plastic yield stress S_p. Then the index is equal to 1.

Finally, a fractional fuel volume change and fractional radial dimensional change of fuel and clad were added to the group 4 output. These are based on instantaneous dimensions relative to the original dimensions at time zero. The diametral changes are calculated for the fuel inner diameter and for the fuel and clad outer diameters. Volume changes are calculated for the fuel only.

Application to Lewis IBM 7094

Storage problems. - Initially, the CYGRO-2 program exceeded the 32 000-word core storage of the IBM 7094. This storage problem was somewhat alleviated by eliminating reference to any of the Westinghouse-Bettis environmental subroutines which were available on the Lewis computer. Elimination of these subroutines would have been done regardless of a core storage problem. Two of the Bettis environmental subroutines had no corresponding Lewis routine. Regular subroutines were made of these (TITLES and LINES) and added to the CYGRO-2 deck. In addition, the subroutine calling the computer time (TICK) was modified in name to call the Lewis timer (TIME1). All the call statements to eliminated subroutines were removed. The subroutine LATON was also split into two subroutines to help decrease required storage. These were called LATON and LATON1. The subroutine LATON1 is simply a section of LATON which allowed an alternate method of reading in the operating history. This resulted in the CYGRO-2 program having a main program and 20 subroutines. To further reduce the required core storage to that amenable to the Lewis computer, four of the subscript ranges of variables used in data storage for restart problems were reduced (FORTRAN names MUF1, MUF2, BUF1, BUF2). These are no longer used for anything in the modified program and could probably be removed if necessary.

The CYGRO-2 program fit onto the computer with only a small amount of storage to spare. It was later found that when further modifications to the program were necessary, core storage continually became a problem. Hence, it was decided to eliminate additional subroutines dealing with tape storage of data because the advantage gained in core storage would be more beneficial, especially since a modified printout option allowed more frequent printout of the parameters. There are currently 13 subroutines in addition to the main program in CYGRO-2. The subroutines are SEND, SEGT, SRAW, STIM, CTAC, SGAS, STEM, SEAS, FINIS, SKEN, LUST, LATON, and LATON1.

General FORTRAN modifications. - A few general modifications were required to make the FORTRAN compatible with the Lewis computer. One of these was the call to the computer timer previously mentioned. Others included redundant parentheses, incorrect reference to read-and-write tapes, incompatible data statements, and an incompatible field width for the A-conversion format on title reading and writing.

Overflows and underflows. - Several modifications were required to eliminate overflow and underflow conditions on the IBM 7094. These always occurred in, or arose from, calculations performed in the subroutine SEGT.

First, the creep relations and the stress-strain relations in subroutine SEGT were originally written in the form

$$e = \exp\left[A \ln 10 + B \ln\left(\frac{S}{1000}\right)\right]$$

where e is the creep rate or the plastic strain for a given stress S. This equation was modified in form to that originally given in reference 1, or

$$e = 10^{A}\left(\frac{S}{1000}\right)^{B}$$

This eliminated underflows that normally occurred when the exponential was evaluated. The second form circumvents this problem by evaluating two lesser exponentials and then directly multiplying them.

Secondly, many of the parameters involved in strain and strain rate calculations were double precisioned. Double precision avoids what would naturally be a computer zero when very small differences are taken between large numbers. These parameters were mostly strain parameters in the subroutine SEGT.

Finally, there are a few critical equations in SEGT where two or more small numbers are calculated and then multiplied together, resulting in an underflow. This is particularly true for very small time steps. This problem can be corrected by checking the magnitude of the variables involved; and if an underflow would occur ($<10^{-38}$), the variable is set equal to zero. (An appropriate control card could accomplish the same thing but only a set number of times before the problem is terminated.) Low values of strain or strain rates, less than 10^{-38}, can be set equal to zero with no ill effect.

SAMPLE PROBLEM

Description of Problem

The CYGRO-2 computer program is being used to predict fuel swelling for uranium mononitride fuel pins. Therefore, the sample problem included here is a UN-fueled fuel pin. The geometry of the fuel pin is as shown in figure 4. It consists of a cylindrical fuel pin with UN fuel and T-111 (Ta-8W-2Hf) clad. The pin is hollow, with a fuel-clad gap of 1.5 mils (3.8×10^{-3} cm) on the radius. The UN fuel is hot pressed and sintered to a density of 96 percent. Power and fuel burnup requirements are 9172 Btu per hour per cubic inch (164 W/cm^3) and 2.77 percent burnup on 50 000 hours. Burnup here refers to fissions only and not total fuel atoms destroyed. An additional heating power of 1 percent is assumed within the clad material (91.72 Btu/(hr)(in.^{3}); 1.64 W/cm^3). Temperature of the clad surface is assumed to be 1720° F (1211 K).

The gas-gap gas is assumed to be helium. The thermal conductivity of helium at 1720° F (1211 K) is approximately 0.0183 Btu per hour per inch per $^{\circ}$F (0.0038 W/(cm)(K))(ref. 9). It was felt that although the xenon fission product would contribute heavily to the gas within the void, the fuel-clad gap would close before an appreciable

error in fuel temperature would occur. It has also been assumed that the interface thermal resistance upon fuel-clad contact is negligible. Therefore, these contact conductivities are very high.

Experimental evidence supports the assumption that only about 5 to 10 percent of the fission products which are gaseous escape from the UN fuel (ref. 10). For this problem 5 percent was assumed. Only one type of bubble has been assumed, although up to five types are possible in the CYGRO-2 program, and the bubble density was assumed to be of the order of 2.7×10^{16} bubbles per cubic inch (1.6×10^{15} bubbles per cm^3). Experimental data of various fuel specimens of a variety of composition has revealed an observable bubble density as low as 5.5×10^{13} bubbles per cubic centimeter to as high as 10^{17} bubbles per cubic centimeter (refs. 11 to 13). Theoretical nucleation densities for inert gas vary between 10^{16} to 10^{18} sites per cubic centimeter (refs. 14 and 15).

Van der Waal's equation-of-state exponents for xenon were used for the gas bubbles. Surface tension on the gas bubble - fuel interface was assumed to be 500 dynes per centimeter (2.855×10^{-3} lb/in.). Gas generation within the bubble is from two sources. First, there is a gaseous fission product generation which is temperature dependent. For this sample problem, only the stable and inert gases were considered. Approximately 15 percent of the fission products are gaseous (0.3 molecule of gas generated for each fission event). Sources for this data are references 16 and 17. A detailed study of resulting fission products is given in reference 18. Most of the nitrogen either recombines with the fuel or combines with other fission products. A small fraction is left uncombined, however, and adds to the gas bubbles. This amount (ref. 19) is temperature dependent but for this sample problem is assumed to be 0.09 molecule per fission event. The total gas generation rate is, therefore, 0.39 molecule per fission.

Solid fission product expansion was assumed to be 0.85 percent solid volume growth per percent burnup. This number has been nominally calculated on a theoretical basis for UO_2 as 0.864 percent growth per percent burnup (ref. 20). Based on 0.3 molecule of fission gas produced per fission and another 1.0 molecule of fission products per fission being used to fill the voids of uranium destroyed, the increase can be shown to be 0.7 percent swelling per percent burnup based only on physical space requirements. Of course, the fission products will not exactly fill the voids. The value chosen for this example problem was 0.85 percent $\Delta V/V$ per percent burnup. Isotropic fuel expansion was assumed throughout.

All the mechanical properties were considered to be independent of fission flux or flux rate. Both the mechanical and appropriate physical properties were assumed to be temperature dependent, with the exception of the Poisson's ratio. Poisson's ratio for uranium mononitride is 0.28. (A value of 0.26 from ref. 21 was revised to a more dense material.) No data exist for Poisson's ratio for T-111 alloy. Therefore, a ratio of 0.35 was assumed because the alloy should not deviate much from the parent material tantalum (ref. 22). Other properties used for T-111 are modulus of elasticity (refs. 23 and 24),

coefficient of thermal expansion (refs. 23 to 26), and the thermal conductivity (refs. 23 and 27). These properties are given in table I. Uranium mononitride properties as used in the program are given in table II. Only one data point for the modulus of UN was available (ref. 28). Temperature dependency was estimated based on the limited amount of known temperature dependency of uranium dioxide and uranium carbide as reported in reference 28. Thermal expansion data are available in references 28 and 29. The source of data on thermal conductivity of UN is reference 30.

The form of equation which describes the stress-against-strain characteristics of a material is

$$\epsilon_p = 10^P \left(\frac{S_p}{1000}\right)^Q$$

where

ϵ_p plastic strain, in./in. (cm/cm)

S_p stress at plastic strain ϵ_p, psi (N/cm^2)

P, Q characteristic exponents, dependent on temperature and flux

Similarly, the form of equation describing creep behavior is

$$\dot{\epsilon}_g = 10^C \left(\frac{S_g}{1000}\right)^G$$

where

$\dot{\epsilon}_g$ equivalent strain rate, in./(in.)(hr)(cm/(cm)(hr))

S_g equivalent stress, psi (N/cm^2)

C, G characteristic exponents, dependent on temperature and flux

The stress-against-strain characteristics of T-111 are shown in figure 5. These curves are the result of both published data (ref. 31) and unpublished TRW data (private communication from K. D. Sheffler, TRW, Inc., Cleveland, Ohio). Since the form of the preceding equation only approximates the true curve, only the characteristic curves and the 0.2 percent yield points are shown in figure 5. The corresponding values of P and Q are given in table II. Creep properties for T-111 were obtained from reference 32. The exponents are tabulated in table III.

There appears to be no data available for the strength of uranium mononitride. It

was assumed that since there was some high-temperature creep data available at 8000 psi (5520 N/cm^2), the yield point must be at least above this. The assumed characteristics and exponents are given in figure 6 and table IV, respectively. Creep characteristics are similar to those in reference 33. The creep equation exponents for UN are given in table IV.

It is not intended that the property values used in the sample problem be interpreted as correct or up to date; they are only the specific values used.

Only one power cycle is considered over a period of 50 000 hours. The temperatures and power come up to maximum in 1 hour and remain there for the duration of the problem, then ramp down to zero power and room temperature in 1 hour. It is assumed that the coolant pressure doubles upon heating and that the gap pressure increases with absolute temperature and ramps linearly while hot from 73.5 to 368.0 psi (50.7 to 253.7 N/cm^2).

Input Data Card Description

A considerable amount of experience has been gained in both debug computations for making modifications to CYGRO-2 and in making studies correlating experimental data with CYGRO-2 predictions (ref. 34). It may be of benefit, therefore, to discuss the input data and the resulting potential problems encountered in using CYGRO-2.

In general, the input is necessarily lengthy and complicated. Because of its length it may take a lengthy period of time to obtain and put the data into useable form. The program user must not only obtain the material's mechanical and physical properties, specify the fuel-pin geometry, and determine the time-dependent conditions, but must correctly model the problem (such as the number and distribution of bubbles) through the many modeling options available. This can be a disadvantage in that the user must be knowledgeable about fuel swelling in order to correctly choose conditions. And, if a new material is being considered, such as some refractory alloy, the required properties are not always known. This further complicates the problem.

Further explanation and comments of input data cards, as they appear in the modified CYGRO-2 program, are given in table V. The program input is given in appendix B.

Sample Problem Results

A FORTRAN statement form of the input data deck is given in appendix B. This particular sample problem has a total of 89 data cards, including a blank end-of-problem card. Also included in appendix B is a sample problem computer printout. This printout contains (1) the identification page; (2) the input data, including both the comment

cards and data cards; (3) a program-calculated table of the plastic stress against strain and creep stress against strain rate; (4) all the calculated parameters at full power (1 hr); (5) an abbreviated printout at the time of fuel-clad contact (18 907 hr); and (6) a printout of all the parameters at the end of life (50 001 hr).

Total fuel swelling for this problem was 5.2 percent, of which 2.35 percent is solid fission product swelling. There is a range in local swelling, ranging from 6.0 percent at the inside node of the fuel to 4.6 percent at the outer node. There is a considerable difference in movement of the fuel between nodes, however. The inside surface of the fuel has been pushed into the central void by about 10 mils (2.54×10^{-2} cm), whereas the outer surface moved out only 1 mil (2.54×10^{-3} cm). For this particular pin the central void serves as a sink for swelling, resulting in very little clad deformation - an ideal situation.

The sample problem ran in a computer time of approximately 10 minutes. Problems involving variations in fuel loading, burnups, irradiation times, cycling, fuel-pin diameters and gaps, and solid or hollow pins have taken from as little as 2 minutes computer time to as high as 60 minutes. Problems which seem to require additional computer times are those involving high gas generation rates and high temperatures. This sample problem used 833 time steps for 50 001 hours.

It is characteristic of the problems run thus far to only load the clad enough to cause plastic flow during a thermal expansion. During the rest of the time the clad is in creep. Running the same problem using different sets of time cards can result in variations in stress when the total strains are the same. This is believed to be due to the stress levels being very sensitive to very small changes in strain and is not significant in determining fuel-pin swelling.

CONCLUDING REMARKS

The CYGRO-2 computer program as initially received was not compatible with the Lewis IBM 7094 computer. The program was subsequently modified such that it would be compatible. It was intended to use the program basically as a design tool after comparing theoretical and experimental fuel swelling. Many computer problems were encountered with the program. Consequently, a debugging and program modification procedure was instituted. Some of these modifications alleviated specific calculational problems, whereas others improved accuracy and computation time.

A discussion of the input data serves to clarify some of the variables that were of questionable nature and magnitude when the program was first utilized. It was found that the tabular functions can, if not carefully set up, result in error and, in some instances, prevent completion of the problem.

A sample problem of a UN fuel pin, with a detailed discussion of the input data, has been included. This sample problem has been utilized to show the changes that have been made in input and output data.

Lewis Research Center,
National Aeronautics and Space Administration,
Cleveland, Ohio, January 13, 1971,
120-27.

APPENDIX A

SYMBOLS

A	coefficient exponent in strain and strain rate equations, replaces C and P
A_{gg}	rate of change of strain rate with respect to stress rate
A_{gt}	strain rate at constant stress
B	stress exponent in strain and strain rate equations, replaces G and Q
C	coefficient exponent in creep equation
C_{lg}	matrix relating equivalent cyclic strain to generalized equivalent strain
e	strain or strain rate
f_{eg}	generalized strain rate function
G	stress exponent in creep equation
P	coefficient exponent in plastic stress-strain equation
Q	stress exponent in plastic stress-strain equation
S	stress
$\dot{S}$	stress rate
ΔS	stress change
S_g	generalized equivalent stress
$\dot{S}_g$	generalized stress rate
S_p	plastic or flow stress
t	time
V	total volume
V_{gh}	gas bubble volume
ϵ	strain
$\dot{\epsilon}$	strain rate
$\Delta\epsilon$	strain change
$\dot{\epsilon}_g$	generalized strain rate
ϵ_l	equivalent plastic strain
ϵ_p	plastic strain

Subscripts:

apparent	apparent value
i	change in variable assumed to take place suddenly at beginning of time step
low	lower value
true	true value
up	upper value

APPENDIX B

SAMPLE PROBLEM INPUT AND OUTPUT

Sample Problem Input Data

```
      SAMPLE PROBLEM - LEWIS MODIFIED CYGRO-2
      TEMP CLAD SURFACE = 1720 F
      T-111 CLAD
      UN FUEL 96 PERCENT DENSE
      FUEL ID = 0.300 OD = 0.621
      3 MIL DIAMETRAL GAP
      PIN OD = 0.750
      INITIAL HOT GAS PRESSURE = 73.5 PSI - FINAL = 368. PSI
      2.77 PERCENT BURNUP 50000 HOURS
      BUBBLE DENSITY = 2.7E+16
      OXYGEN CONTENT OF FUEL 400-500 PPM
      5 PERCENT GAS LEAKAGE
      0.85 PERCENT SOLID GROWTH PER PERCENT BURNUP
13
    30.0     0.0    10.0  1000.0   1.0-6   1.0-4   1.0-2     0.5     900
     0.0     1.0     1.0     1.0     1.0     0.0                     901
  1000.0     1.0     1.0     1.0     1.0     0.0                     902
  3000.0     1.0     1.0     1.0     1.0     0.0                     903
  1.83-2 1.00+10 1.00+10 1.00+10 1.854+4 1.420+34.630+10   460       904
                          2000.0  1.00-3                  5000.0     905
       1       0       1       0       1       0       0       1     906
       0  1.00-3       0     1.0     1.3       0    1000    1000     907
      11       1     1.0     1.0       2  9172.0     0.0 2.855-3    1000
  0.1500                                                            1001
  0.1530                                                            1001
```

NASA-C-836 (REV. 9-14-59)

```
  0.1550                                                            1001
  0.1605 -                                                          1001
  0.1819                                                            1001
  0.2033                                                            1001
  0.2248                                                            1001
  0.2462                                                            1001
  0.2676                                                            1001
  0.2890                                                            1001
  0.3105                                                            1001
  6.45-8 1.426-7  2.00-6    0.04    1.00 27.0+16       0.27.0+16    1002
    1.00    1.00    1.00   0.333   0.333   0.333                    1003
     0.0  6000.0 10000.0                                            1004
       1     1.0       3     1.0       6     1.0      11     1.0    1005
    32.0  4.67-6  31.0+6    0.28   0.770     1.0     1.0     1.0    1010
         -30.000   5.902 -22.699    20.0                            1011
         -30.000   5.902 -22.699    20.0                            1012
         -30.000   5.902 -22.699    20.0                            1013
   932.0  4.67-6  30.3+6    0.28   0.982     1.0     1.0     1.0    1020
         -15.131   5.902 -22.053    20.0                            1021
         -15.131   5.902 -22.053    20.0                            1022
         -15.131   5.902 -22.053    20.0                            1023
  1832.0  5.06-6  28.5+6    0.28   1.160     1.0     1.0     1.0    1030
         -8.5344   5.902 -21.405    20.0                            1031
         -8.5344   5.902 -21.405    20.0                            1032
         -8.5344   5.902 -21.405    20.0                            1033
```

NASA-C-836 (REV. 9-14-59)

1 2 3 4 5	6	7 8 9 10 11 12	13 14 15 16 17 18	19 20 21 22 23 24	25 26 27 28 29 30	31 32 33 34 35 36	37 38 39 40 41 42	43 44 45 46 47 48	49 50 51 52 53 54	55 56 57 58 59 60	61 62 63 64 65 66	67 68 69 70 71 72	73 74 75 76 77 78 79 80
273	2	.0 5.	34-6	22.8+6	0.	28 1	.248	1.0	1	.0	1.0	1040	
		-5.	6583	5.902	-20.7	59	20.0					1041	
		-5.	6583	5.902	-20.7	59	20.0					1042	
		-5.	6583	5.902	-20.7	59	20.0					1043	
		6	0	1.0	1	.0	2	91.72	0	.0 2.8	55-3	2000	
0.	3	12										2001	
0.	3	17										2001	
0.	3	32										2001	
0.	3	47										2001	
0.	3	62										2001	
0.	3	75										2001	
1	.	00	1.00	1.00	0.3	33 0	.333	0.333				2003	
	0	.0 600	0.0 1	0000.0								2004	
		1	1.0	2	1	.0	3	1.0		6	1.0	2005	
3	2	.0 3.	00-6	26.0+6	0.	35	2.00	1.0	1	.0	1.0	2010	
		-30	.000	3.692	-31.2	70 1	5.10					2011	
		-30	.000	3.692	-31.2	70 1	5.10					2012	
		-30	.000	3.692	-31.2	70 1	5.10					2013	
183	2	.0 3.	65-6	23.0+6	0.	35	2.81	1.0	1	.0	1.0	2020	
		-10	.474	3.692	-25.4	27 1	5.10					2021	
		-10	.474	3.692	-25.4	27 1	5.10					2022	
		-10	.474	3.692	-25.4	27 1	5.10					2023	
240	0	.0 3.	92-6	22.0+6	0.	35	3.00	1.0	1	.0	1.0	2030	
		-7.	2300	3.692	-23.9	00 1	5.00					2031	
		-7.	2300	3.692	-23.9	00 1	5.00					2032	

NASA-C-836 (REV. 9-14-59)

1 2 3 4 5	6	7 8 9 10 11 12	13 14 15 16 17 18	19 20 21 22 23 24	25 26 27 28 29 30	31 32 33 34 35 36	37 38 39 40 41 42	43 44 45 46 47 48	49 50 51 52 53 54	55 56 57 58 59 60	61 62 63 64 65 66	67 68 69 70 71 72	73 74 75 76 77 78 79 80
		-7.	2300	3.692	-23.9	00 1	5.10					2033	
273	2	.0 4.	08-6	21.4+6	0.	35	3.05	1.0	1	.0	1.0	2040	
		-5.	8776	3.692	-22.6	64 1	5.10					2041	
		-5.	8776	3.692	-22.6	64 1	5.10					2042	
		-5.	8776	3.692	-22.6	64 1	5.10					2043	
							15.10	15.0			70.0	.001	
			3	.020-3	3.020	-3	73.5	30.0	1	.0 17	20.0	1	
4.7	0	-5	3	.020-3	3.020	-1	74.1	30.0	1	.0 17	20.0	100	
2.3	5	-4	3	.020-3	1.510		76.5	30.0	1	.0 17	20.0	500	
4.7	0	-4	3	.020-3	3.020		79.4	30.0	1	.0 17	20.0	1000	
1.1	8	-2	3	.020-3	75.50	2	21.0	30.0	1	.0 17	20.0	25000	
2.3	5	-2	3	.020-3	151.0	3	68.0	30.0	1	.0 17	20.0	50000	
2.3	5	-2			151.0		75.0	15.0			70.0	50001	

NASA-C-836 (REV. 9-14-59)

Sample Problem Output

```
$TCP            TIME=30,PAGES=200,FORMS=PLAIN
$OVRFLW         CONTINUE
$MAJUND         CONTINUE
$ZERDIV         CONTINUE
$IBJOB          GO,NOSOURCE



0     SAMPLE PROBLEM - LEWIS MODIFIED CYGRO-2

0     TEMP CLAD SURFACE = 1720 F

0     T-111 CLAD

0     UN FUEL 96 PERCENT DENSE

0     FUEL ID = 0.300 OD = 0.621

0     3 MIL DIAMETRAL GAP

0     PIN OD = 0.750

0     INITIAL HOT GAS PRESSURE = 73.5 PSI - FINAL = 368. PSI

0     2.77 PERCENT BURNUP 50000 HOURS

0     BUBBLE DENSITY 2.7E+16

0     OXYGEN CONTENT OF FUEL 400-500 PPM

0     5 PERCENT GAS LEAKAGE

0     0.85 PERCENT SOLID GROWTH PER PERCENT BURNUP



3

 WCS          F(1)         F(2)         F(3)         FDOT(1)      FDOT(2)      FDOT(3)      0            9.00  + 2
 3.0000E+01   0.           1.0000E+01   1.0000E+03   1.0000E-06   1.0000E-04   1.0000E-02   5.0000E-01   9.0000E+02

 TG(K)        DFT(1,K)     DFT(2,K)     DFT(3,K)     RGASN(K)     ZUYKB        0            0            9.0K  + 2
 0.           1.0000E+00   1.0000E+00   1.0000E+00   1.0000E+00   0.           0.           0.           9.0100E+02
 1.0000E+03   1.0000E+00   1.0000E+00   1.0000E+00   1.0000E+00   0.           0.           0.           9.0200E+02
 3.0000E+03   1.0000E+00   1.0000E+00   1.0000E+00   1.0000E+00   0.           0.           0.           9.0300E+02

 CGAP         HGAP         HNOGAP       HWATER       R(VDW)       A(VDW)       B(VDW)       TABS         9.04  + 2
 1.8300E-02   1.0000E+10   1.0000E+10   1.0000E+10   1.8540E+04   1.4200E+03   4.6300E+10   4.6000E+02   9.0400E+02

VAN DER WAALS LOWER TEMPERATURE LIMIT IS  -20.

 FCORE        FCON(R)      FCON(Z)      DS(MAX)      DE(MAX)      RPLUG        QPLUG        TPLUG        9.05  + 2
-0.          -0.          -0.           2.0000E+03   1.0000E-03  -0.          -0.           5.0000E+03   9.0500E+02

 SGMIN        MPQ          MCORE        MGAS         MGL          EDOGS        MFILE        PFILE        9.06  + 2
 1.0000E+00   0.           1.0000E+00   0.           1.0000E+00   0.           0.           1.0000E+00   9.0600E+02

        -1

 MCEE         DVMAX        HIST         RAP          RBP          MAXC         MMM          NNN          9.07  + 2
 0.           1.0000E-03   0.           1.0000E+00   1.3000E+00   0.           1.0000E+03   1.0000E+03   9.0700E+02


               ----MEAT  PROPERTIES----

 NR           NG           RSC          RSP          MCGPQ        QGMAX        EZ           S.TEN.       1.000 + 3
 1.1000E+01   1.0000E+00   1.0000E+00   1.0000E+00   2.0000E+00   9.1720E+03   0.           2.8550E-03   1.0000E+03
```

RADIUS(KR)	SR(KE)	SC(KE)	SZ(KE)	EGC(KE)	EGZ(KE)	EG(KE)	EV(KE)	I.001 + 3
1.5000E-01	-0.	-0.	-0.	-0.	-0.	-0.	-0.	1.0010E+03
1.5300E-01	-0.	-0.	-0.	-0.	-0.	-0.	-0.	1.0010E+03
1.5500E-01	-0.	-0.	-0.	-0.	-0.	-0.	-0.	1.0010E+03
1.6050E-01	-0.	-0.	-0.	-0.	-0.	-0.	-0.	1.0010E+03
1.8190E-01	-0.	-0.	-0.	-0.	-0.	-0.	-0.	1.0010E+03
2.0330E-01	-0.	-0.	-0.	-0.	-0.	-0.	-0.	1.0010E+03
2.2480E-01	-0.	-0.	-0.	-0.	-0.	-0.	-0.	1.0010E+03
2.4620E-01	-0.	-0.	-0.	-0.	-0.	-0.	-0.	1.0010E+03
2.6760E-01	-0.	-0.	-0.	-0.	-0.	-0.	-0.	1.0010E+03
2.8900E-01	-0.	-0.	-0.	-0.	-0.	-0.	-0.	1.0010E+03
3.1050E-01	-0.	-0.	-0.	-0.	-0.	-0.	-0.	1.0010E+03

MOLES(KG)	AM(KG)	BM(KG)	VH(KG)	V(KG)	NH(KG)	MNHT(KG)	NHT(KG)	I.002 + 3
6.4500E-08	1.4260E-07	2.0000E-06	4.0000E-02	1.0000E+00	2.7000E+16	-0.	2.7000E+16	1.0020E+03

RALPHA(R)	RALPHA(C)	RALPHA(Z)	RV(R)	RV(C)	RV(Z)	0	0	I.003 + 3
1.0000E+00	1.0000E+00	1.0000E+00	3.3300E-01	3.3300E-01	3.3300E-01	-0.	-0.	1.0030E+03

P(1)	P(2)	P(3)	0	0	0	0	0	I.004 + 3
-0.	6.0000E+03	1.0000E+04	-0.	-0.	-0.	-0.	-0.	1.0040E+03

KR(=1)	RQ(1)	KR	RQ(KR)	KR	RQ(KR)	KR	RQ(KR)	I.005 + 3
1.0000E+00	1.0000E+00	3.0000E+00	1.0000E+00	6.0000E+00	1.0000E+00	1.1000E+01	1.0000E+00	1.0050E+03

TEMPT(J)	ALPHAT(J)	ET(J)	NUT(J)	CT(J)	RVP(1,J)	RVP(2,J)	RVP(3,J)	I.0J0 + 3
0	CFT(K,J)	GFT(K,J)	PFT(K,J)	QFT(K,J)	0	0	0	I.0JK + 3
3.2000E+01	4.6700E-06	3.1000E+07	2.8000E-01	7.7000E-01	1.0000E+00	1.0000E+00	1.0000E+00	1.0100E+03
-0.	-3.0000E+01	5.9020E+00	-2.2699E+01	2.0000E+01	-0.	-0.	-0.	1.0110E+03
-0.	-3.0000E+01	5.9020E+00	-2.2699E+01	2.0000E+01	-0.	-0.	-0.	1.0120E+03
-0.	-3.0000E+01	5.9020E+00	-2.2699E+01	2.0000E+01	-0.	-0.	-0.	1.0130E+03
9.3200E+02	4.6700E-06	3.0300E+07	2.8000E-01	9.8200E-01	1.0000E+00	1.0000E+00	1.0000E+00	1.0200E+03
-0.	-1.5131E+01	5.9020E+00	-2.2053E+01	2.0000E+01	-0.	-0.	-0.	1.0210E+03
-0.	-1.5131E+01	5.9020E+00	-2.2053E+01	2.0000E+01	-0.	-0.	-0.	1.0220E+03
-0.	-1.5131E+01	5.9020E+00	-2.2053E+01	2.0000E+01	-0.	-0.	-0.	1.0230E+03
1.8320E+03	5.0600E-06	2.8500E+07	2.8000E-01	1.1600E+00	1.0000E+00	1.0000E+00	1.0000E+00	1.0300E+03
-0.	-8.5344E+00	5.9020E+00	-2.1405E+01	2.0000E+01	-0.	-0.	-0.	1.0310E+03
-0.	-8.5344E+00	5.9020E+00	-2.1405E+01	2.0000E+01	-0.	-0.	-0.	1.0320E+03
-0.	-8.5344E+00	5.9020E+00	-2.1405E+01	2.0000E+01	-0.	-0.	-0.	1.0330E+03
2.7320E+03	5.3400E-06	2.2800E+07	2.8000E-01	1.2480E+00	1.0000E+00	1.0000E+00	1.0000E+00	1.0400E+03
-0.	-5.6583E+00	5.9020E+00	-2.0759E+01	2.0000E+01	-0.	-0.	-0.	1.0410E+03
-0.	-5.6583E+00	5.9020E+00	-2.0759E+01	2.0000E+01	-0.	-0.	-0.	1.0420E+03
-0.	-5.6583E+00	5.9020E+00	-2.0759E+01	2.0000E+01	-0.	-0.	-0.	1.0430E+03

----CLAD PROPERTIES----

NR	NG	RSC	RSP	MCGPQ	QGMAX	EZ	S.TEN.	I.000 + 3
6.0000E+00	0.	1.0000E+00	1.0000E+00	2.0000E+00	9.1720E+01	0.	2.8550E-03	2.0000E+03

RADIUS(KR)	SR(KE)	SC(KE)	SZ(KE)	EGC(KE)	EGZ(KE)	EG(KE)	EV(KE)	I.001 + 3
3.1200E-01	-0.	-0.	-0.	-0.	-0.	-0.	-0.	2.0010E+03
3.1700E-01	-0.	-0.	-0.	-0.	-0.	-0.	-0.	2.0010E+03
3.3200E-01	-0.	-0.	-0.	-0.	-0.	-0.	-0.	2.0010E+03
3.4700E-01	-0.	-0.	-0.	-0.	-0.	-0.	-0.	2.0010E+03
3.6200E-01	-0.	-0.	-0.	-0.	-0.	-0.	-0.	2.0010E+03
3.7500E-01	-0.	-0.	-0.	-0.	-0.	-0.	-0.	2.0010E+03

RALPHA(R)	RALPHA(C)	RALPHA(Z)	RV(R)	RV(C)	RV(Z)	0	0	I.003 + 3
1.0000E+00	1.0000E+00	1.0000E+00	3.3300E-01	3.3300E-01	3.3300E-01	0.	0.	2.0030E+03

P(1)	P(2)	P(3)	0	0	0	0	0	I.004 + 3
0.	6.0000E+03	1.0000E+04	-0.	-0.	-0.	-0.	-0.	2.0040E+03

KR(=1)	RQ(1)	KR	RQ(KR)	KR	RQ(KR)	KR	RQ(KR)	I.005 + 3
1.0000E+00	1.0000E+00	2.0000E+00	1.0000E+00	3.0000E+00	1.0000E+00	6.0000E+00	1.0000E+00	2.0050E+03

TEMPT(J)	ALPHAT(J)	ET(J)	NUT(J)	CT(J)	RVP(1,J)	RVP(2,J)	RVP(3,J)	I.0J0 + 3
0	CFT(K,J)	GFT(K,J)	PFT(K,J)	QFT(K,J)	0	0	0	I.0JK + 3
3.2000E+01	3.0000E-06	2.6000E+07	3.5000E-01	2.0000E+00	1.0000E+00	1.0000E+00	1.0000E+00	2.0100E+03
-0.	-3.0000E+01	3.6920E+00	-3.1270E+01	1.5100E+01	-0.	-0.	-0.	2.0110E+03
-0.	-3.0000E+01	3.6920E+00	-3.1270E+01	1.5100E+01	-0.	-0.	-0.	2.0120E+03
-0.	-3.0000E+01	3.6920E+00	-3.1270E+01	1.5100E+01	-0.	-0.	-0.	2.0130E+03
1.8320E+03	3.6500E-06	2.3000E+07	3.5000E-01	2.8100E+00	1.0000E+00	1.0000E+00	1.0000E+00	2.0200E+03
-0.	-1.0474E+01	3.6920E+00	-2.5427E+01	1.5100E+01	-0.	-0.	-0.	2.0210E+03
-0.	-1.0474E+01	3.6920E+00	-2.5427E+01	1.5100E+01	-0.	-0.	-0.	2.0220E+03
-0.	-1.0474E+01	3.6920E+00	-2.5427E+01	1.5100E+01	-0.	-0.	-0.	2.0230E+03

2.4000E+03	3.9200E-06	2.2000E+07	3.5000E-01	3.0000E+00	1.0000E+00	1.0000E+00	1.0000E+00	2.0300E+03
-0.	-7.2300E+00	3.6920E+00	-2.3900E+01	1.5100E+01	-0.	-0.	-0.	2.0310E+03
-0.	-7.2300E+00	3.6920E+00	-2.3900E+01	1.5100E+01	-0.	-0.	-0.	2.0320E+03
-0.	-7.2300E+00	3.6920E+00	-2.3900E+01	1.5100E+01	-0.	-0.	-0.	2.0330E+03

2.7320E+03	4.0800E-06	2.1400E+07	3.5000E-01	3.0500E+00	1.0000E+00	1.0000E+00	1.0000E+00	2.0400E+03
-0.	-5.8776E+00	3.6920E+00	-2.2664E+01	1.5100E+01	-0.	-0.	-0.	2.0410E+03
-0.	-5.8776E+00	3.6920E+00	-2.2664E+01	1.5100E+01	-0.	-0.	-0.	2.0420E+03
-0.	-5.8776E+00	3.6920E+00	-2.2664E+01	1.5100E+01	-0.	-0.	-0.	2.0430E+03

KM	KT	KF	SP(0.001)	SP(0.002)	SP(0.005)	SP(0.010)	SP(0.020)	SP(0.050)	SP(0.100)	SP(0.200)	SP(0.500)	SP(1.000)
1	1											
		1	9659.	10000.	10469.	10838.	11220.	11746.	12160.	12589.	13179.	13644.
		2	9659.	10000.	10469.	10838.	11220.	11746.	12160.	12589.	13179.	13644.
		3	9659.	10000.	10469.	10838.	11220.	11746.	12160.	12589.	13179.	13644.
1	2											
		1	8967.	9283.	9718.	10061.	10416.	10904.	11289.	11687.	12235.	12666.
		2	8967.	9283.	9718.	10061.	10416.	10904.	11289.	11687.	12235.	12666.
		3	8967.	9283.	9718.	10061.	10416.	10904.	11289.	11687.	12235.	12666.
1	3											
		1	8322.	8616.	9020.	9338.	9667.	10120.	10477.	10847.	11355.	11756.
		2	8322.	8616.	9020.	9338.	9667.	10120.	10477.	10847.	11355.	11756.
		3	8322.	8616.	9020.	9338.	9667.	10120.	10477.	10847.	11355.	11756.
1	4											
		1	7726.	7998.	8373.	8669.	8974.	9395.	9726.	10069.	10541.	10913.
		2	7726.	7998.	8373.	8669.	8974.	9395.	9726.	10069.	10541.	10913.
		3	7726.	7998.	8373.	8669.	8974.	9395.	9726.	10069.	10541.	10913.
2	1											
		1	74505.	78005.	82885.	86778.	90854.	96538.	101073.	105821.	112441.	117723.
		2	74505.	78005.	82885.	86778.	90854.	96538.	101073.	105821.	112441.	117723.
		3	74505.	78005.	82885.	86778.	90854.	96538.	101073.	105821.	112441.	117723.
2	2											
		1	30564.	32000.	34002.	35599.	37271.	39603.	41463.	43411.	46127.	48293.
		2	30564.	32000.	34002.	35599.	37271.	39603.	41463.	43411.	46127.	48293.
		3	30564.	32000.	34002.	35599.	37271.	39603.	41463.	43411.	46127.	48293.
2	3											
		1	24216.	25354.	26940.	28205.	29530.	31378.	32852.	34395.	36546.	38263.
		2	24216.	25354.	26940.	28205.	29530.	31378.	32852.	34395.	36546.	38263.
		3	24216.	25354.	26940.	28205.	29530.	31378.	32852.	34395.	36546.	38263.
2	4											
		1	20058.	21000.	22314.	23362.	24459.	25990.	27210.	28489.	30271.	31693.
		2	20058.	21000.	22314.	23362.	24459.	25990.	27210.	28489.	30271.	31693.
		3	20058.	21000.	22314.	23362.	24459.	25990.	27210.	28489.	30271.	31693.

KM	KT	KF	SC(1.E-6)	SC(1.E-5)	SC(1.E-4)	SC(0.001)	SC(0.01)	SC(0.1)	SC(1.0)	SC(10.0)
1	1									
		1	1.16525E+07	1.72128E+07	2.54265E+07	3.75596E+07	5.54823E+07	8.19575E+07	1.21066E+08	1.78837E+08
		2	1.16525E+07	1.72128E+07	2.54265E+07	3.75596E+07	5.54823E+07	8.19575E+07	1.21066E+08	1.78837E+08
		3	1.16525E+07	1.72128E+07	2.54265E+07	3.75596E+07	5.54823E+07	8.19575E+07	1.21066E+08	1.78837E+08
1	2									
		1	3.52454E+04	5.20639E+04	7.69079E+04	1.13607E+05	1.67818E+05	2.47898E+05	3.66191E+05	5.40930E+05
		2	3.52454E+04	5.20639E+04	7.69079E+04	1.13607E+05	1.67818E+05	2.47898E+05	3.66191E+05	5.40930E+05
		3	3.52454E+04	5.20639E+04	7.69079E+04	1.13607E+05	1.67818E+05	2.47898E+05	3.66191E+05	5.40930E+05
1	3									
		1	2.68790E+03	3.97052E+03	5.86519E+03	8.66395E+03	1.27982E+04	1.89053E+04	2.79266E+04	4.12527E+04
		2	2.68790E+03	3.97052E+03	5.86519E+03	8.66395E+03	1.27982E+04	1.89053E+04	2.79266E+04	4.12527E+04
		3	2.68790E+03	3.97052E+03	5.86519E+03	8.66395E+03	1.27982E+04	1.89053E+04	2.79266E+04	4.12527E+04
1	4									
		1	8.75194E+02	1.29282E+03	1.90973E+03	2.82102E+03	4.16717E+03	6.15565E+03	9.09304E+03	1.34321E+04
		2	8.75194E+02	1.29282E+03	1.90973E+03	2.82102E+03	4.16717E+03	6.15566E+03	9.09304E+03	1.34321E+04
		3	8.75194E+02	1.29282E+03	1.90973E+03	2.82102E+03	4.16717E+03	6.15566E+03	9.09304E+03	1.34321E+04
2	1									
		1	3.16622E+09	5.90742E+09	1.10218E+10	2.05641E+10	3.83677E+10	7.15849E+10	1.33560E+11	2.49191E+11
		2	3.16622E+09	5.90742E+09	1.10218E+10	2.05641E+10	3.83677E+10	7.15849E+10	1.33560E+11	2.49191E+11
		3	3.16622E+09	5.90742E+09	1.10218E+10	2.05641E+10	3.83677E+10	7.15849E+10	1.33560E+11	2.49191E+11
2	2									
		1	1.62858E+04	3.03854E+04	5.66919E+04	1.05774E+05	1.97348E+05	3.68204E+05	6.86981E+05	1.28174E+06
		2	1.62858E+04	3.03854E+04	5.66919E+04	1.05774E+05	1.97348E+05	3.68204E+05	6.86981E+05	1.28174E+06
		3	1.62858E+04	3.03854E+04	5.66919E+04	1.05774E+05	1.97348E+05	3.68204E+05	6.86981E+05	1.28174E+06
2	3									
		1	2.15354E+03	4.01799E+03	7.49660E+03	1.39869E+04	2.60961E+04	4.86892E+04	9.08423E+04	1.69490E+05
		2	2.15354E+03	4.01799E+03	7.49660E+03	1.39869E+04	2.60961E+04	4.86892E+04	9.08423E+04	1.69490E+05
		3	2.15354E+03	4.01799E+03	7.49660E+03	1.39869E+04	2.60961E+04	4.86892E+04	9.08423E+04	1.69490E+05
2	4									
		1	9.26504E+02	1.72863E+03	3.22522E+03	6.01748E+03	1.12272E+04	2.09472E+04	3.90825E+04	7.29186E+04
		2	9.26504E+02	1.72863E+03	3.22522E+03	6.01748E+03	1.12272E+04	2.09472E+04	3.90825E+04	7.29186E+04
		3	9.26504E+02	1.72863E+03	3.22522E+03	6.01748E+03	1.12272E+04	2.09472E+04	3.90825E+04	7.29186E+04

EVS(MEAT)	EVS(CLAD)	FDOT	F	P(GAP)	P(WATER)	QG/QGMAX	T(WATER)	TIME
-0.	-0.	-0.	-0.	1.5000E+01	1.5000E+01	-0.	7.0000E+01	1.0000E-03
-0.	-0.	3.0200E-03	3.0200E-03	7.3500E+01	3.0000E+01	1.0000E+00	1.7200E+03	1.0000E+00

KTIME= 10 DTIME= 0.9780E-01 LAPSED SECONDS= 5.783 TIME= 1.0000

RADII.... RA(M)= 0.15130 RB(M)= 0.31318 R(GAP)= 0.54472E-03 RB(C)= 0.37707

FORCES... FCORE= 0 FCON(R)= 0 FCON(Z)= 0

STRAINS.. EZ(M)= 0.8615E-02 EZ(C)= 0.5510E-02 EMAX(M)= 0.1565E-03 EMAX(C)= 0.1000E-07

STRESS... SMAX(M)= 8367.7 SMAX(C)= 1546.5

PARAMS... DV/V = 0.02611 DD/D(C)= 0.00553 DD/D(F-OD)= 0.00863 DD/D(F-ID)= 0.00864
PLASTIC FLOW INDEX = 1 1 1 1 0 0 0 0 1 1 0 0 0 0 0

KM	KR	TEMP	RADIUS	DEG/DT	SP	PB	T(AVE)	//	EV	VH	VH(1)	VH(2)	VH(3)	VH(4)	VH(5)
1	1	1872.70	0.15130		0.74825E-03		7438.43		4966.26		1784.44				
		-0.23544E-05	0.39998E-01		0.39998E-01		0		0		0		0		
1	2	1872.66	0.15432		0.73475E-03		7405.64		5082.51		1784.39				
		-0.25630E-05	0.39997E-01		0.39997E-01		0		0		0		0		
1	3	1872.59	0.15634		0.68449E-03		7364.89		5041.55		1784.18				
		-0.24736E-05	0.39998E-01		0.39998E-01		0		0		0		0		
1	4	1872.22	0.16189		0.15695E-03		6847.19		5423.54		1782.21				
		-0.24140E-05	0.39998E-01		0.39998E-01		0		0		0		0		
1	5	1868.44	0.18348		0.88742E-05		5891.99		4727.57		1776.99				
		-0.13858E-05	0.39999E-01		0.39999E-01		0		0		0		0		
1	6	1851.24	0.20507		0.20562E-06		4979.48		3274.84		1768.60				
		-0.49174E-06	0.40000E-01		0.40000E-01		0		0		0		0		
1	7	1850.81	0.22676		0.12361E-07		4736.78		1296.60		1757.30				
		-0.11176E-06	0.40000E-01		0.40000E-01		0		0		0		0		
1	8	1837.47	0.24835		0.20037E-05		5489.93		-1182.18		1743.26				
		-0.14901E-07	0.40000E-01		0.40000E-01		0		0		0		0		
1	9	1821.29	0.26993		0.21662E-03		6980.35		-3751.70		1726.58				
		-0.74506E-08	0.40000E-01		0.40000E-01		0		0		0		0		
1	10	1802.38	0.29151		0.17172E-03		7664.07		-5210.53		1707.27				
		-0.74506E-08	0.40000E-01		0.40000E-01		0		0		0		0		
1	11	1780.69	0.31318		0		0		0		0				
		0	0		0		0		0		0		0		
2	1	1743.23	0.31373		0.16960E-11		15523.3		1115.52		1660.38				
		0	0		0		0		0		0		0		
2	2	1741.23	0.31875		0.21001E-12		15551.9		705.898		1656.66				
		0	0		0		0		0		0		0		
2	3	1735.41	0.33384		0.41637E-15		15593.6		112.711		1651.24				
		0	0		0		0		0		0		0		
2	4	1729.83	0.34892		0.13366E-12		15633.8		-457.006		1646.04				
		0	0		0		0		0		0		0		
2	5	1724.47	0.36400		0.10404E-11		15670.1		-967.711		1641.36				
		0	0		0		0		0		0		0		
2	6	1720.00	0.37707		0		0		0		0				
		0	0		0		0		0		0		0		

KM	KE	ET-6	SR	SC	SZ	SG //	EG	EGR	EGC	EGZ	EL	SL(R-C)	SL(C-Z)	SL(Z-R)
1	1	28.595	-181.25	-7448.2		-7284.3	7186.4							
		0.9781E-04	0.9780E-04	-0.4939E-04		-0.4841E-04	0.9781E-04				0.1007E+05	-182.45		-9890.3
1	2	28.595	-378.12	-7465.4		-7419.3	7064.3							
		0.8953E-04	0.8952E-04	-0.4409E-04		-0.4543E-04	0.8953E-04				9634.4	-20.655		-9613.7
1	3	28.596	-391.35	-7311.2		-7437.2	6983.7							
		0.8015E-04	0.8010E-04	-0.3798E-04		-0.4212E-04	0.8015E-04				9171.1	204.80		-9375.9
1	4	28.600	-870.58	-7321.1		-8095.5	6870.5							
		0.1860E-04	0.1848E-04	-0.7518E-05		-0.1096E-04	0.1860E-04				6946.2	839.99		-7786.2
1	5	28.610	-1487.1	-5605.0		-7104.8	5038.1							
		0.9133E-06	0.8710E-06	-0.2282E-06		-0.6428E-06	0.9133E-06				4138.9	1507.7		-5646.6
1	6	28.627	-1769.7	-3132.7		-4931.9	2747.2							
		0.3112E-07	0.1721E-07	0.1990E-08		-0.1920E-07	0.3112E-07				1363.3	1799.6		-3162.9
1	7	28.649	-1754.4	-174.52		-1964.8	1694.9							
		0.1124E-07	-0.5272E-09	0.1238E-08		-0.7110E-09	0.1124E-07				-1579.9	1790.3		-210.37
1	8	28.677	-1438.9	3252.3		1736.6	4146.6							
		0.2101E-06	-0.1899E-06	0.1496E-06		0.4026E-07	0.2101E-06				-4697.7	1517.8		3179.9
1	9	28.711	-951.46	6550.3		5667.5	7101.6							
		0.2493E-04	-0.2475E-04	0.1488E-04		0.9867E-05	0.2493E-04				-8260.2	978.70		7281.5
1	10	28.749	-362.71	8004.9		8005.0	8367.7							
		0.1565E-03	-0.1564E-03	0.8198E-04		0.7440E-04	0.1565E-03				-0.1294E+05	145.29		0.1279E+05
2	1	23.286	-89.378	-1553.9		-1706.6	1546.5							
		0.1000E-07	0.1668E-12	-0.7040E-13		-0.9644E-13	0.1000E-07				1464.5	152.70		-1617.2
2	2	23.292	-115.89	-910.42		-1093.5	900.14							
		0.1000E-07	0.2022E-13	-0.6990E-14		-0.1323E-13	0.1000E-07				794.53	183.07		-977.61
2	3	23.301	-130.83	-4.7111		-202.93	173.77							
		0.1000E-07	0	0		-0	0.1000E-07				-126.12	198.22		-72.093
2	4	23.310	-105.79	826.78		651.40	858.42							
		0.1000E-07	-0.1287E-13	0.8436E-14		0.4429E-14	0.1000E-07				-932.56	175.37		757.19
2	5	23.318	-57.658	1545.5		1418.2	1543.4							
		0.1000E-07	-0.1025E-12	0.5703E-13		0.4546E-13	0.1000E-07				-1603.2	127.30		1475.9

KM	KE	KG	DFT	PGAS	PA	SG(AVE)	SP	SC	RA	VA	VPC	NH(T)	MOLES
1	1	1	1.00E+00	6.73E+01	-8.01E+03	6.05E+03	8.65E+03	1.13E+08	7.07E-07	4.00E-02	-1.82E-01	2.70E+16	6.47E-08
1	2	1	1.00E+00	6.73E+01	-8.01E+03	6.10E+03	8.65E+03	1.08E+08	7.07E-07	4.00E-02	-1.90E-01	2.70E+16	6.47E-08
1	3	1	1.00E+00	6.73E+01	-8.01E+03	6.08E+03	8.65E+03	1.10E+08	7.07E-07	4.00E-02	-1.87E-01	2.70E+16	6.47E-08
1	4	1	1.00E+00	6.73E+01	-8.01E+03	6.26E+03	8.65E+03	9.89E+07	7.07E-07	4.00E-02	-1.79E-01	2.70E+16	6.47E-08
1	5	1	1.00E+00	6.71E+01	-8.01E+03	5.93E+03	8.66E+03	1.40E+08	7.07E-07	4.00E-02	-1.50E-01	2.70E+16	6.47E-08
1	6	1	1.00E+00	6.69E+01	-8.01E+03	5.26E+03	8.66E+03	2.92E+08	7.07E-07	4.00E-02	-1.12E-01	2.70E+16	6.47E-08
1	7	1	1.00E+00	6.65E+01	-8.01E+03	4.34E+03	8.67E+03	9.10E+08	7.07E-07	4.00E-02	-7.64E-02	2.70E+16	6.47E-08
1	8	1	1.00E+00	6.61E+01	-8.01E+03	3.18E+03	8.68E+03	5.26E+09	7.07E-07	4.00E-02	-4.82E-02	2.70E+16	6.47E-08
1	9	1	1.00E+00	6.56E+01	-8.01E+03	1.98E+03	8.69E+03	7.06E+10	7.07E-07	4.00E-02	-2.71E-02	2.70E+16	6.47E-08
1	10	1	1.00E+00	6.50E+01	-8.01E+03	1.30E+03	8.71E+03	7.64E+11	7.07E-07	4.00E-02	-2.83E-02	2.70E+16	6.47E-08

0	KRDT	KCTAC	JERKS	RQPLUG
	0	10	0	1.0000E+00

```
EVS(MEAT)   EVS(CLAD)   FDOT        F           P(GAP)      P(WATER)    QG/QGMAX    T(WATER)    TIME
4.7000E-04 -0.          3.0200E-03  3.0200E+00  7.9400E+01  3.0000E+01  1.0000E+00  1.7200E+03  1.0000E+03
1.1800E-02 -0.          3.0200E-03  7.5500E+01  2.2100E+02  3.0000E+01  1.0000E+00  1.7200E+03  2.5000E+04

    KTIME=        53       DTIME=      316.46              LAPSED SECONDS=    41.317          TIME=  18906.9277

   RADII....              RA(M)=    0.15156     RB(M)=    0.31373     R(GAP)=    0               RB(C)=    0.37708

   FORCES...              FCORE=      0             FCON(R)=     0             FCON(Z)=      0

   STRAINS..              EZ(M)=     0.1041E-01     EZ(C)=     0.5514E-02     EMAX(M)=     0.4666E-03     EMAX(C)=     0.3302E-06

   STRESS...              SMAX(M)=       652.13         SMAX(C)=       1963.2

   PARAMS...              DV/V =  0.03154     DD/D(C)= 0.00555     DD/D(F-OD)= 0.01041     DD/D(F-ID)= 0.01042
   PLASTIC FLOW INDEX =    0 0 0 0 0 0 0 0 0 0 0 0 0 0 0 0

EVS(MEAT)   EVS(CLAD)   FDOT        F           P(GAP)      P(WATER)    QG/QGMAX    T(WATER)    TIME
2.3500E-02 -0.          3.0200E-03  1.5100E+02  3.6800E+02  3.0000E+01  1.0000E+00  1.7200E+03  5.0000E+04
2.3500E-02 -0.         -0.          1.5100E+02  7.5000E+01  1.5000E+01 -0.          7.0000E+01  5.0001E+04

    KTIME=       833       DTIME=      0.4501E-01          LAPSED SECONDS=   618.100          TIME=  50001.0000

   RADII....              RA(M)=    0.14000     RB(M)=    0.31172     R(GAP)=    0.67439E-03     RB(C)=    0.37532

   FORCES...              FCORE=      0             FCON(R)=     0             FCON(Z)=      0

   STRAINS..              EZ(M)=     0.2489E-02     EZ(C)=     0.1803E-03     EMAX(M)=     0.1125          EMAX(C)=     0.1588E-02

   STRESS...              SMAX(M)=       0.1405E+05     SMAX(C)=       1517.7

   PARAMS...              DV/V =  0.05217     DD/D(C)= 0.00084     DD/D(F-OD)= 0.00394     DD/D(F-ID)=-0.06669
   PLASTIC FLOW INDEX =    0 1 0 0 0 0 0 0 0 1 0 0 0 0 0

 KM KR    TEMP  RADIUS  DEG/DT      SP          PB      T(AVE)  //    EV      VH   VH(1)   VH(2)   VH(3)   VH(4)   VH(5)

 1  1   70.0002       0.14000       0.50514E-22   12147.7       -8465.04       111.940
          0.60082E-01   0.76582E-01   0.76582E-01   0             0              0              0

 1  2   70.0002       0.14339       0.12879E-21   12125.5       -8980.41       111.938
          0.59721E-01   0.76221E-01   0.76221E-01   0             0              0              0

 1  3   70.0002       0.14565       0.23643E-22   12093.6       -8072.34       111.929
          0.59538E-01   0.76038E-01   0.76038E-01   0             0              0              0

 1  4   70.0002       0.15182       0.72291E-23   11985.9       -7589.60       111.847
          0.57620E-01   0.74120E-01   0.74120E-01   0             0              0              0

 1  5   70.0002       0.17546       0.49574E-24   11834.2       -6074.03       111.635
          0.55954E-01   0.72454E-01   0.72454E-01   0             0              0              0

 1  6   70.0002       0.19869       0.11004E-25   11699.6       -4012.85       111.306
          0.54021E-01   0.70521E-01   0.70521E-01   0             0              0              0

 1  7   70.0002       0.22172       0.90928E-26   11577.8       -1448.21       110.873
          0.51950E-01   0.68450E-01   0.68450E-01   0             0              0              0

 1  8   70.0002       0.24443       0.56144E-24   11466.6        1570.14       110.346
          0.49921E-01   0.66421E-01   0.66421E-01   0             0              0              0

 1  9   70.0001       0.26696       0.10178E-22   11362.3        5022.48       109.730
          0.47847E-01   0.64347E-01   0.64347E-01   0             0              0              0

 1 10   70.0001       0.28935       0.54126E-20   11263.2        8901.66       109.029
          0.45805E-01   0.62305E-01   0.62305E-01   0             0              0              0

 1 11   70.0001       0.31172       0             0              0              0
          0             0             0             0             0              0              0
```

2	1	70.3000	0.31240	0.14973E-28	73992.5	618.598	107.788	
		0	0	0	0	0	0	0
2	2	70.3000	0.31738	0.11157E-29	73618.2	366.517	107.673	
		0	0	0	0	0	0	0
2	3	70.3000	0.33236	0	73065.0	-6.94080	107.505	
		0	0	0	0	0	0	0
2	4	70.3000	0.34735	0.66397E-29	72526.7	-372.738	107.343	
		0	0	0	0	0	0	0
2	5	70.3000	0.36233	0.38927E-28	72033.9	-711.012	107.199	
		0	0	0	0	0	0	0
2	6	70.3000	0.37532	0	0	0	0	
		0	0	0	0	0	0	0

KM	KE	ET-6	SR	SC	SZ	SG //	EG	EGR	EGC	EGZ	EL	SL(R-C)	SL(C-Z)	SL(Z-R)
1	1	30.938		81.373		0.1299E+05	0.1235E+05		0.1260E+05					
		0.1125		0.1043		-0.8687E-01	-0.1746E-01		0.1118		0.3930E+07	-0.1431E+07		-0.2499E+07
1	2	30.938		339.67		0.1391E+05	0.1271E+05		0.1302E+05					
		0.1087		0.1008		-0.8341E-01	-0.1735E-01		0.1077		0.3785E+07	-0.1361E+07		-0.2423E+07
1	3	30.938		677.91		0.1168E+05	0.1188E+05		0.1111E+05					
		0.1027		0.9588E-01		-0.7860E-01	-0.1728E-01		0.1022		0.3588E+07	-0.1265E+07		-0.2323E+07
1	4	30.938		1565.4		0.1009E+05	0.1114E+05		9092.9					
		0.8558E-01		0.8091E-01		-0.6426E-01	-0.1666E-01		0.8545E-01		0.2986E+07	-0.9828E+06		-0.2003E+07
1	5	30.938		2429.0		6801.6	9009.7		5800.9					
		0.6629E-01		0.6367E-01		-0.4758E-01	-0.1609E-01		0.6621E-01		0.2290E+07	-0.6518E+06		-0.1638E+07
1	6	30.938		2718.7		3307.5	6024.4		3054.1					
		0.5270E-01		0.5130E-01		-0.3589E-01	-0.1541E-01		0.5265E-01		0.1798E+07	-0.4252E+06		-0.1373E+07
1	7	30.939		2591.1		-498.95	2256.8		2937.2					
		0.4272E-01		0.4204E-01		-0.2737E-01	-0.1467E-01		0.4267E-01		0.1435E+07	-0.2648E+06		-0.1170E+07
1	8	30.939		2135.4		-4637.9	-2212.7		5944.1					
		0.3532E-01		0.3491E-01		-0.2100E-01	-0.1392E-01		0.3515E-01		0.1160E+07	-0.1484E+06		-0.1012E+07
1	9	30.940		1407.9		-9124.4	-7366.0		9772.5					
		0.2974E-01		0.2920E-01		-0.1606E-01	-0.1314E-01		0.2925E-01		0.9441E+06	-0.6207E+05		-0.8820E+06
1	10	30.940		442.20		-0.1399E+05	-0.1318E+05		0.1405E+05					
		0.2539E-01		0.2452E-01		-0.1217E-01	-0.1235E-01		0.2452E-01		0.7712E+06	2898.7		-0.7741E+06
2	1	25.874		-84.863		-1451.4	-321.39		1265.0					
		0.1588E-02		-0.1452E-02		0.1283E-02	0.1687E-03		0.1588E-02		-0.4580E+05	0.1809E+05		0.2771E+05
2	2	25.874		-113.52		-801.40	-185.73		654.77					
		0.1470E-02		-0.1350E-02		0.1177E-02	0.1728E-03		0.1469E-02		-0.4291E+05	0.1671E+05		0.2620E+05
2	3	25.874		-124.67		112.20	33.311		208.91					
		0.1310E-02		-0.1212E-02		0.1035E-02	0.1778E-03		0.1310E-02		-0.3900E+05	0.1486E+05		0.2414E+05
2	4	25.874		-97.070		947.44	268.96		917.96					
		0.1170E-02		-0.1092E-02		0.9101E-03	0.1815E-03		0.1170E-02		-0.3557E+05	0.1325E+05		0.2232E+05
2	5	25.875		-44.687		1671.9	507.98		1517.7					
		0.1055E-02		-0.9908E-03		0.8072E-03	0.1836E-03		0.1054E-02		-0.3273E+05	0.1192E+05		0.2081E+05

KM	KE	KG	DFT	PGAS	PA	SG(AVE)	SP	SC	RA	VA	VPC	NH(T)	MOLES
1	1	1	1.00E+00	1.26E+03	-5.24E+03	1.86E+03	9.93E+03	2.30E+30	8.78E-07	7.66E-02	4.00E-02	2.70E+16	2.06E-05
1	2	1	1.00E+00	1.27E+03	-5.25E+03	2.15E+03	9.93E+03	1.13E+30	8.77E-07	7.62E-02	4.61E-02	2.70E+16	2.06E-05
1	3	1	1.00E+00	1.27E+03	-5.25E+03	1.62E+03	9.93E+03	4.47E+30	8.76E-07	7.60E-02	3.47E-02	2.70E+16	2.06E-05
1	4	1	1.00E+00	1.29E+03	-5.28E+03	1.31E+03	9.93E+03	1.27E+31	8.69E-07	7.41E-02	2.75E-02	2.70E+16	2.06E-05
1	5	1	1.00E+00	1.31E+03	-5.31E+03	4.29E+02	9.93E+03	3.07E+33	8.62E-07	7.25E-02	8.73E-03	2.70E+16	2.06E-05
1	6	1	1.00E+00	1.33E+03	-5.35E+03	7.47E+02	9.93E+03	2.04E+32	8.54E-07	7.05E-02	-1.54E-02	2.70E+16	2.06E-05
1	7	1	1.00E+00	1.37E+03	-5.38E+03	2.18E+03	9.94E+03	1.09E+30	8.46E-07	6.85E-02	-4.36E-02	2.70E+16	2.06E-05
1	8	1	1.00E+00	1.40E+03	-5.41E+03	3.83E+03	9.94E+03	7.06E+28	8.37E-07	6.64E-02	-7.54E-02	2.70E+16	2.06E-05
1	9	1	1.00E+00	1.45E+03	-5.44E+03	5.67E+03	9.94E+03	1.05E+28	8.29E-07	6.43E-02	-1.30E-01	2.70E+16	2.06E-05
1	10	1	1.00E+00	1.51E+03	-5.46E+03	7.70E+03	9.94E+03	2.41E+27	8.20E-07	6.23E-02	-2.56E-01	2.70E+16	2.06E-05

0	KRDT	KCTAC	JERKS	RQPLUG
	32	1131	0	1.0000E-06

EVS(MEAT)	EVS(CLAD)	FDOT	F	P(GAP)	P(WATER)	QG/QGMAX	T(WATER)	TIME
2.3500E-02	-0.	-0.	1.5100E+02	7.5000E+01	1.5000E+01	-0.	7.0000E+01	5.0001E+04

BLANK CARD END OF PROBLEM *****

KRDT	KCTAC	KTIME	TINY	DELTA	JERKS	RDT	STEPS/SEC.	MINUTES
32	1131	833	1.0000E-07	4.5010E-02	0	1.0000E+00	1.3442E+00	1.0328E+01

END OF OUTPUT

01 EXIT IN SKEN

APPENDIX C

MODIFIED CYGRO-2 SUBROUTINES AND MAJOR FUNCTIONS

Subroutine	Function
SWELL	main program: controls all input data card reading
STIM	main calculational program: controls all calculations, selects time increments, initializes, and prints output
STEM	calculates heat generation and temperature distributions
SEND	sets up interpolation of time cards and controls interpolation of properties table
SGAS	gas bubble calculations, solid swelling
SKEN	reads time cards, input transition to other subroutines
SRAW	input transition between reading subroutine and storing subroutine
LATON	reads all input data
LATON1	former part of subroutine LATON
FINIS	writes 'end of output'
LUST	interpolation procedure for tables
SEAS	finishes calculating stress and strain increments and adds to value at start of time step, interpolates material properties as a function of temperature, prints some output, performs matrix manipulations, and serves a transition for gas bubble calculations
CTAC	calculates contact loads between rings, performs matrix manipulations
SEGT	calculates creep rates and plastic flow rates, interpolates properties as a function of flux or flux rate

REFERENCES

1. Friedrich, C. M.; and Guilinger, W. H.: CYGRO-2: A FORTRAN IV Computer Program for Stress Analysis of the Growth of Cylindrical Fuel Elements with Fission Gas Bubbles. Rep. WAPD-TM-547, Bettis Atomic Power Lab., 1966.

2. Goldberg, I.; Lynn, L. L.; and Sphar, C. D.: FIGRO: FORTRAN-IV Digital Computer Program for the Analysis of Fuel Swelling and Calculation of Temperature in Bulk-Oxide Cylindrical Fuel Elements. Rep. WAPD-TM-618, Bettis Atomic Power Lab., 1966.

3. Friedrich, C. M.: CYGRO - Stress Analysis of the Growth of Concentric Cylinders. Rep. WAPD-TM-514, Bettis Atomic Power Lab., Oct. 1965.

4. Friedrich, C. M.: CYGRO-1 Stress Analysis of the Growth of Concentric Cylinders. Rep. WAPD-TM-514, Add. No. 1, Bettis Atomic Power Lab., July 1966.

5. Duncombe, E.; Meyer, J. E.; and Coffman, W. A.: Comparisons with Experiment of Calculated Dimensional Changes and Failure Analysis of Irradiated Bulk Oxide Fuel Test Rods Using the CYGRO-1 Computer Program. Rep. WAPD-TM-583, Bettis Atomic Power Lab., Sept. 1966.

6. Duncombe, E.: A Procedure for Analysis of Zircaloy-Clad Bulk Oxide Rods Using the CYGRO-1 Computer Program. Rep. WAPD-TM-583, Add. No. 1, Bettis Atomic Power Lab., Apr. 1967.

7. Duncombe, E.: Analysis of Void Migration, Clad Collapse and Fuel Cracking in Bulk Oxide Fuel Rods. Rep. WAPD-TM-794, Bettis Atomic Power Lab., July 1968.

8. McCracken, Daniel D.; and Dorn, William S.: Numerical Methods and FORTRAN Programming. John Wiley & Sons, Inc., 1964.

9. Andrew, A. D.; and Calvert, C. S.: Thermal Conductivity and Viscosity of Neon, Helium, Argon, and Xenon, and Their Binary Mixtures. Rep. GE-TM-66-7-9, General Electric Co. (AEC Rep. TID-24636), Apr. 4, 1966.

10. Weaver, S. C.; Scott, J. L.; Senn, R. L.; and Montgomery, B. H.: Effects of Irradiation on Uranium Nitride Under Space-Reactor Conditions. Rep. ORNL-4461, Oak Ridge National Lab., Oct. 1969.

11. Kulcinski, G. L.; Leggett, R. D.; Hann, C. R.; and Mastel, B.: Fission Gas Induced Swelling in Uranium at High Temperatures and Pressures. J. Nucl. Mat., vol. 30, no. 3, Apr. 1969, pp. 303-313.

12. Katz, O. M.: Fission Gas Bubbles in Fractured UO_2 Chips. J. Nucl. Mat., vol. 31, no. 3, July 1969, pp. 323-326.

13. Hudson, B.: The Post-Irradiation Annealing Behavior of Fission Gas Bubbles in Various Purities of Uranium. J. Nucl. Mat., vol. 27, no. 1, July 1969, pp. 54-63.

14. Nelson, R. S.: The Stability of Gas Bubbles in An Irradiation Environment. J. Nucl. Mat., vol. 31, no. 2, June 1969, pp. 153-161.

15. Eyre, B. L.; and Bullough, R.: The Formation and Behaviour of Gas Bubbles in a Non-Uniform Temperature Enviornment. J. Nucl. Mat., vol. 26, no. 3, June 1969, pp. 249-266.

16. McIntosh, A. B.; and Heal, T. J., eds.: Materials for Nuclear Engineers. Interscience Publ., Inc., 1960, p. 39.

17. Kaufman, Albert R., ed.: Nuclear Reactor Fuel Elements; Metallurgy and Fabrication. Interscience Publ., Inc., 1962, p. 295.

18. Paulson, Walter A.; and Springborn, Roy H.: Estimation of Fission-Product Gas Pressure in Uranium Dioxide Ceramic Fuel Elements. NASA TN D-4823, 1968.

19. Allbutt, M.; and Dell, R. M.: Chemical Aspects of Nitride, Phosphide, and Sulphide Fuels. J. Nucl. Mat., vol. 24, no. 1, Oct. 1967, pp. 1-20.

20. Anselin, F.; and Baily, W. E.: The Role of Fission Products in the Swelling of Irradiated UO_2 and $(U, Pu)O_2$ Fuels. Trans. Amer. Nucl. Soc., vol. 10, no. 1, June 1967, pp. 103-104.

21. Taylor, K. M.; and McMurtry, C. H.: Synthesis and Fabrication of Refractory Uranium Compounds. Rep. ORO-400, Carborundum Co., Feb. 1961.

22. Köster, Werner; and Franz, H.: Poisson's Ratio for Metals and Alloys. Metallurg. Rev., vol. 6, no. 21, 1961, pp. 1-55.

23. Wolf, J.; and Brown, W. F., Jr., eds.: Aerospace Structural Metal Handbook. Volume IIA. Non-Ferrous Alloys. Belfour Stulen, Inc. (AFML-TR-68-115), 1970.

24. Anon.: Elastic Modulus and Thermal Expansion of Tantalum T-111 Alloy. Westinghouse Electric Corp., Astronuclear Lab., Feb. 1964.

25. Schmidt, F. F.; and Ogden, H. R.: The Engineering Properties of Tantalum and Tantalum Alloys. DMIC Rep. 189, Battelle Memorial Inst., Sept. 13, 1963.

26. Anon.: Columbium, Tantalum, and Tungsten Alloys. Technical Information. Vol. 3. Wah Chang Corp. (AEC Rep. NP-16657, vol. 3), 1966.

27. Jun, C. K.; and Hoch, M.: Thermal Conductivity and Total Emittance of Tantalum, Tungsten, Rhenium, Ta-10W, T111, T222, and W-25Re in the Temperature Range 1500 to 2800 K. High Temperature Technology. Butterworth and Co., Ltd., 1969, pp. 535-545.

28. Burdi, G. F., ed.: SNAP Technology Handbook. Volume III. Refractory Fuels and Claddings. Rep. NAA-SR-8617, Vol. III, Atomics International, Apr. 30, 1965.

29. De Crescente, M. A.; Freed, M. S.; and Caplow, S. D.: Uranium Nitride Fuel Development - SNAP-50. Rep. PWAC-488, Pratt & Whitney Aircraft, Oct. 1965.

30. Hayes, B. A.; and DeCrescente, M. A.: Thermal Conductivity and Electrical Resistivity of Uranium Mononitride. Rep. PWAC-481, Pratt & Whitney Aircraft, Oct. 1965.

31. Sheffler, K. D.; Sawyer, J. C.; and Steigerwald, E. A.: Mechanical Behavior of Tantalum-Base T-111 Alloy at Elevated Temperature. Rep. TRW-ER-7365, TRW Equipment Labs., Mar. 1969.

32. Maag, William L.; and Mattson, William F.: Statistical Analysis of High-Temperature Creep-Rate Data for Alloys of Tantalum, Molybdenum, and Columbium. NASA TN D-5424, 1969.

33. Vandervoort, Richard R.; Barmore, Willis L.; and Cline, Carl F.: Compressive Creep of Polycrystalline Uranium Mononitride in Nitrogen. Tran. AIME, vol. 242, no. 7, July 1968, pp. 1466-1467.

34. Davison, H. W.; and Fiero, I. B.: Calculation of the Radiation Induced Swelling of Uranium Mononitride Using the Digital Computer Program CYGRO-2 (U). NASA TM X-2224, 1970.

TABLE I. - PROPERTIES OF T-111

[Poisson's ratio, 0.35.]

Temperature		Modulus of elasticity		Coefficient of expansion		Conductivity	
^{o}F	K	psi	N/cm^2	in./(in.)(^{o}F)	cm/(cm)(K)	Btu/(hr)(in.)(^{o}F)	W/(cm)(K)
32	273	26.0×10^{6}	18.2×10^{6}	3.00×10^{-6}	5.40×10^{-6}	2.00	0.415
1832	1273	23.0	16.1	3.65	6.57	2.81	.583
2400	1589	22.0	15.4	3.92	7.06	3.00	.623
2732	1773	21.4	15.0	4.08	7.34	3.05	.633

TABLE II. - PROPERTIES OF UN

[Poisson's ratio, 0.28.]

Temperature		Modulus of elasticity		Coefficient of expansion		Conductivity	
^{o}F	K	psi	N/cm^2	in./(in.)(^{o}F)	cm/(cm)(K)	Btu/(hr)(in.)(^{o}F)	W/(cm)(K)
32	273	31.0×10^{6}	21.7×10^{6}	4.67×10^{-6}	8.40×10^{-6}	0.770	0.160
932	773	30.3	21.2	4.67	8.40	.982	.204
1832	1273	28.5	19.9	5.06	9.11	1.160	.241
2732	1773	22.8	15.9	5.34	9.61	1.248	.259

TABLE III. - STRESS-STRAIN AND CREEP

EXPONENTS OF T-111

Temperature		Stress-strain exponents		Creep exponents	
^{o}F	K	P	Q	C	G
32	273	-31.270	15.10	-30.000	3.692
1832	1273	-25.427	↓	-10.474	↓
2400	1589	-23.900	↓	-7.230	↓
2732	1773	-22.665	↓	-5.878	↓

TABLE IV. - STRESS-STRAIN AND CREEP

EXPONENTS FOR UN

Temperature		Stress-strain exponents		Creep exponents	
^{o}F	K	P	Q	C	G
32	273	-22.699	20.0	-30.000	5.902
932	773	-22.053	↓	-15.131	↓
1832	1273	-21.405	↓	-8.534	↓
1732	1773	-20.759	↓	-5.658	↓

TABLE V. - INPUT DATA CARDS

Card	Comments
Comment cards	These are the first cards to appear after the $DATA card. The modified CYGRO-2 allows any number of comments on as many cards as are necessary to completely describe the problem. These words can fill columns 3 to 72. The last comment card must contain a numerical number greater than 0 in columns 1 to 2. The next card must be the 900 card.
900	The first variable on the 900 card is the plastic flow rate exponent. Allowing the exponent to approach plus infinity would make flow instantaneous. However, this is not practicable on the computer. On the IBM 7094 an exponent is limited in magnitude and it was found that a value of 30 to 35 was satisfactory. This value allowed sufficiently rapid relaxation of stresses, whereas larger exponents occasionally created run stoppage.
	The run limit specified in this version of CYGRO-2 was and is not utilized. It is simply erased when the next card is read.
	In all tabulated input data, only the range between maximum and minimum specified values is used. If at any time the tabulated variable has an incompatible range as compared with a calculated variable, the end points are used; no extrapolation beyond the table ever occurs.
90K K = 1, 2, 3	The gas leakage function is difficult to evaluate for problems where cycling takes place. The function on page 19 reference 1 must be integrated over the life of the fuel pin to determine the correct coefficient or function if a specified amount of gas release is required.
904	The film coefficient between fuel and clad can create problems if the gap coefficient and no-gap coefficient are greatly different. Since the temperature level in the fuel changes suddenly upon contact (it gets cooler), the fuel would thermally contract away from the clad. An oscillation can be set up where the program stays in the "twilight zone" for a period of time.
905	The maximum allowable stress and strain change (ΔS and $\Delta\epsilon$, respectively) are not computer-time restrictive based solely on magnitude. There is some optimum ΔS and $\Delta\epsilon$ for each problem. For example, a problem ran with $\Delta\epsilon$ = 0.001 in./in. (0.001 cm/cm) and ΔS = 1000, 2000, and 10 000 psi (689, 1379, and 6895 N/cm^2) ran the quickest with ΔS = 2000 psi (1379 N/cm^2). Too large an increment can set up instabilities which take longer to straighten out. Maximum allowable temperature in the plug must be approached with caution. The CYGRO-2 program calculates a temperature distribution; if the maximum is exceeded, the volumetric heat generation rate specified on card 1000 is proportioned down such that the centerline or plug temperature is exactly the specified maximum. There may be occasions when this is not desired.

TABLE V. - CONTINUED. INPUT DATA CARDS

Card	Comments
906	The calculation option, S_{gmin}, on the form of S_g partial derivatives represents a minimum stress at which this option is utilized. As a stress, it is not critical that it equal 1. Only a small number is required for the same result.
	Fuel-plug contact requirement is necessary for the case of solid fuel pins. It is this variable which allows the user to specify a solid or hollow fuel pin in addition to radii specification.
	Input-output option, M_{gas}, determines whether to expect only one I002 card or a card for each individual ring. Some of the data specified on more than one I002 card are not stored; these are discussed under the I002 card comments. The E_{dogs} option for solid fuel swelling must be used with the pressure factor R_{vp} on card I0J0. This allows the user to lump all sources of swelling into one modified solid swelling if desired. This approach to modeling fuel swelling may be desirable if data on swelling as a function of pressure and temperature are available.
907	Two new variables have been added to this card. These variables are counters dealing with the printout of the calculations and appear in the seventh and eighth data fields, columns 57 to 72. They are print frequencies. Each is given a number, m and n, respectively. Every m^{th} time step a printout of group 4 (ref. 1) data occurs, and every n^{th} step a printout of groups 4 to 7 occurs. This feature easily allows more of the calculations to be printed for cases where long periods of time occur between history cards.
I000 I = 1, 2	Two factors or multipliers are used to modify the material mechanical properties around the gas bubbles. One is a creep stress factor and the other is a plastic stress factor; they appear in the third and fourth fields of the card. The plastic stress factor appears as a multiplier on the 0.2 percent yield stress. Since, for bubble equilibrium calculations, strain hardening is not considered, this provides an alternate method of inputing some average strain hardening. The creep stress factor is a multiplier also utilized in determining the stress level around the bubble. For bubbles calculations the stress is never allowed to exceed the yield; and if yield is reached, the extent to which plastic flow extends into the material region around the bubbles must be determined. A plastic stress factor greater than 1 increases the yield point and, consequently decreases the plastic zone (although the average stress may be higher). A creep stress factor greater than 1 increases the plastic zone. It also increases the apparent stress level in the creep zone. These factors can be arbitrarily used to increase or decrease fuel swelling. However, for UN fuel, use of factors equal to 1 has resulted in satisfactory agreement between experimental and calculated fuel swelling.
	Full-power heat generation rate must be the reference power level if the fuel pin is cycled.
I002 I = 1, 2	These cards describe the gas bubble conditions in the fuel and clad. If all the rings are the same, there need to be only as many cards as there are bubble types. Some of these conditions may be varied from ring to ring. If this is done, there should be a card for each ring.

TABLE V. - CONCLUDED. INPUT DATA CARDS

Card	Comments
I002 (continued)	The fission coefficient was subscripted in the modified CYGRO-2 such that it may also vary from ring to ring. This will allow, in effect, a variable gas generation rate in the radial direction. Total solid volume associated with each bubble type is not ring dependent within the program. This is a fractional value, and in most cases should total up to 1.0. However, it is not mathematically necessary.
I004 I = 1, 2	Gas pressures used in this tabulation must be specified and they must be in three distinctly different values. Even if the pressure factor is not utilized, the three specified pressures cannot all be zero or the same.
I005 I = 1, 2	Any number of node points, from 2 to 4, may be specified for a constant or variable heat generation, as a function of the radius index. However, the complete range of the index must be covered in nondecreasing order.
I0JK I = 1, 2 J = 1, 2, 3, 4 K = 1, 2, 3	It is characteristic of most materials that the creep coefficient decreases (in absolute value) nonlinearly with increasing temperature while the exponent remains constant or nearly constant. Interpolation between two temperatures in the table always results in a creep exponent that is too large. The result is an apparently stronger material. It can appear stronger by a few orders in magnitude in creep rate. This situation, it has been found, is best alleviated by setting up the table around an operating temperature or temperature range. In this way the range over which interpolation occurs is much smaller, and the resulting error is also much smaller. Caution must be used, in any case, to prevent the operating temperature from falling midpoint between two widely separated temperatures in the table. An example of spacing the temperatures in the table in a more useful manner is given in the sample problem for the cladding.
	Another interpolation problem was encountered in the temperature-dependent plastic stress-strain exponents. It at first seemed appropriate to solve for the exponents at each temperature in the table by forcing the function through two points - the 0.2 percent yield point and another point at much higher plastic strain which would be representative of maximum strains expected for the problem. However, the resulting coefficients and exponents usually behave rather badly; that is, they do not plot as a smooth function with temperature. The resulting interpolation can generate a pair of coefficients and exponents which do not correctly model the material behavior, but can result in a 0.2 percent yield, for example, which is outside the range of intended interpolation. Sometimes this can cause an instability in the stresses and strains which results in termination of the computer problem. It has been found that the best results are obtained when the following procedure is used: First, obtain the coefficients at the expected operating temperature; then, keeping the stress exponent constant or nearly so, vary the coefficient such that the function will pass through the 0.2 percent yield point at each temperature level. Keeping the stress exponent constant and only varying the coefficient results in a curve showing more strain hardening at lower temperatures than at higher temperatures, which is usually the way most materials behave. If, however, it is desired to vary both coefficients and exponent to properly model the material, caution should be exercised to avoid instabilities in interpolation.
	The first data field utilized on this card is the second field. The first field is left blank.

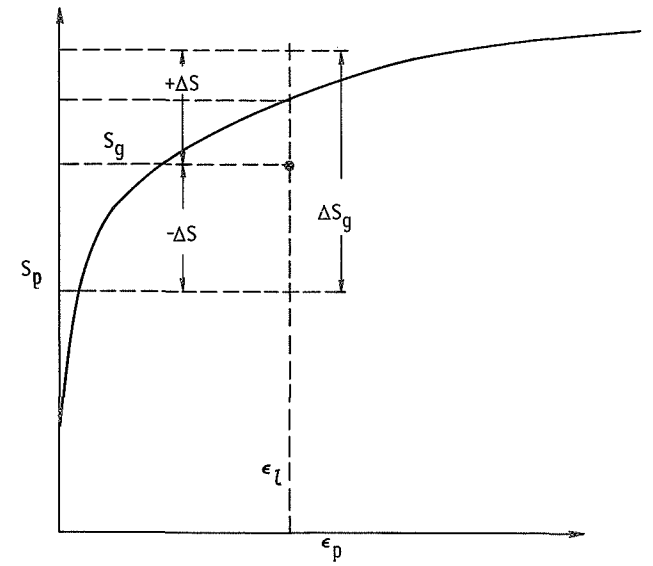

(a) Plastic stress diagram.

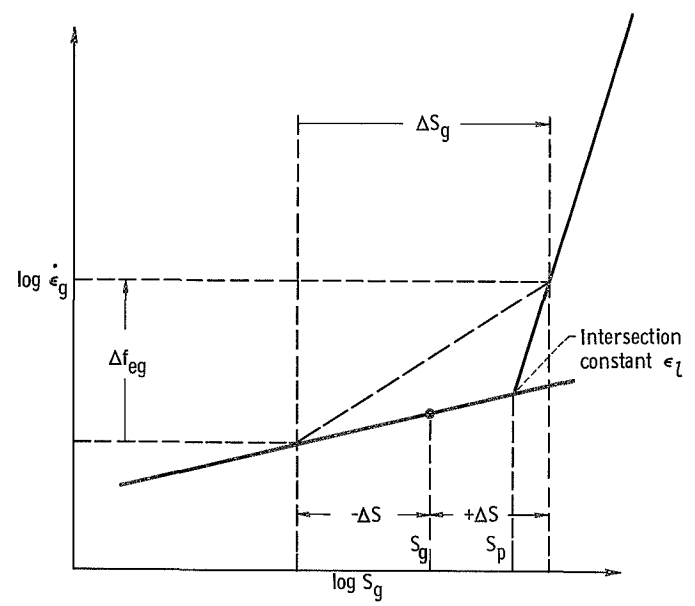

(b) Creep - plastic flow diagram.

Figure 1. - Evaluation of rate of change of strain rate with respect to change in stress $\partial f_{eg}/\partial S_g$ at constant strain.

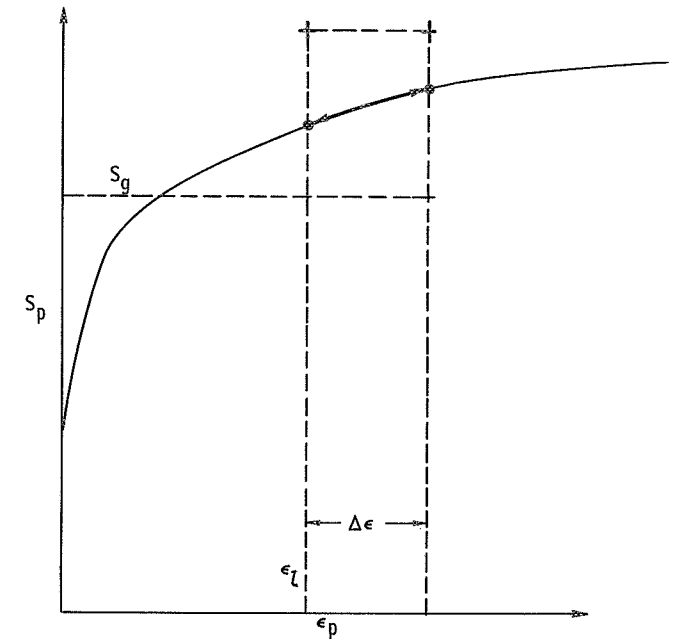

(a) Plastic stress diagram.

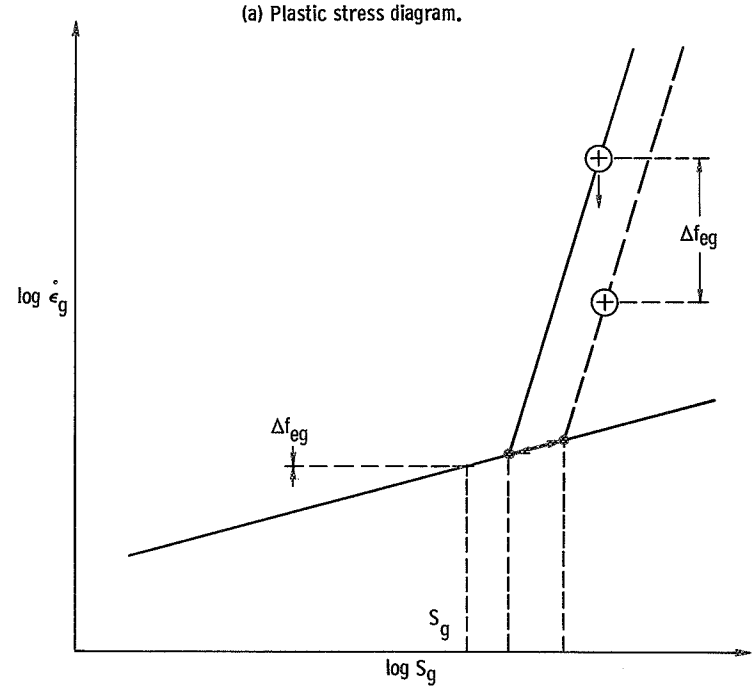

(b) Creep - plastic flow diagram.

Figure 2. - Evaluation of rate of change of strain rate with respect to change in total strain $\partial f_{eg}/\partial \epsilon_l$ at constant stress.

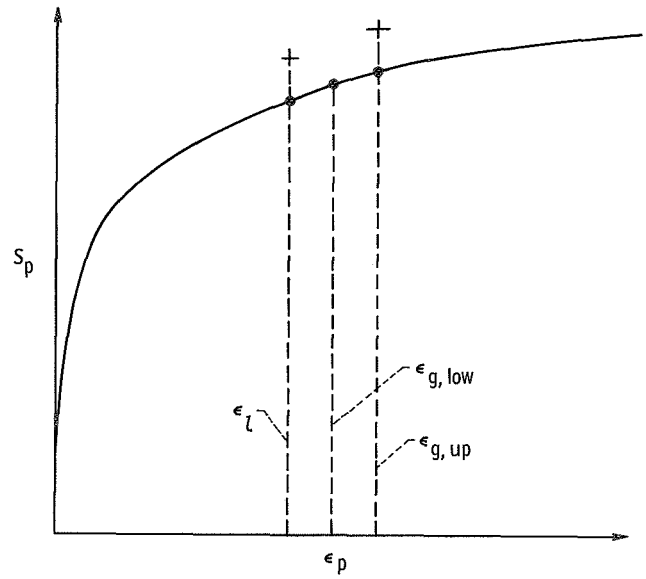

(a) Plastic stress diagram.

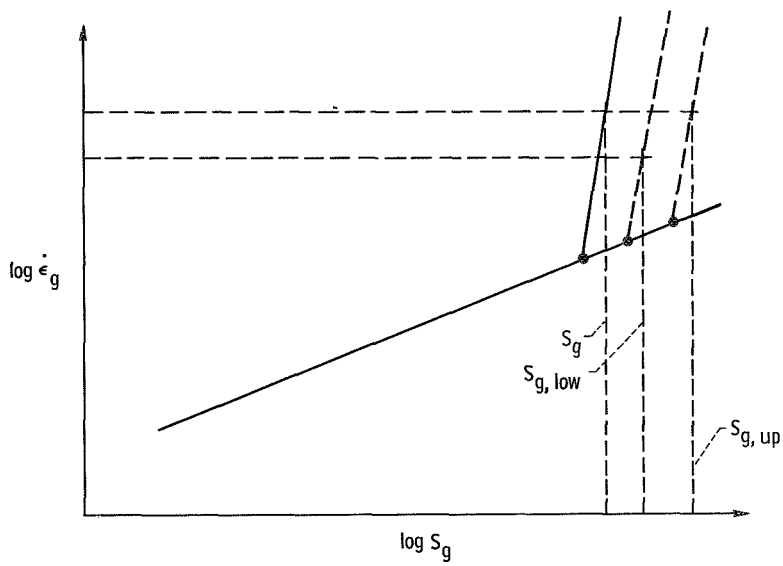

(b) Creep - plastic flow diagram.

Figure 3. - Evaluation of rate of change of strain with respect to stress.

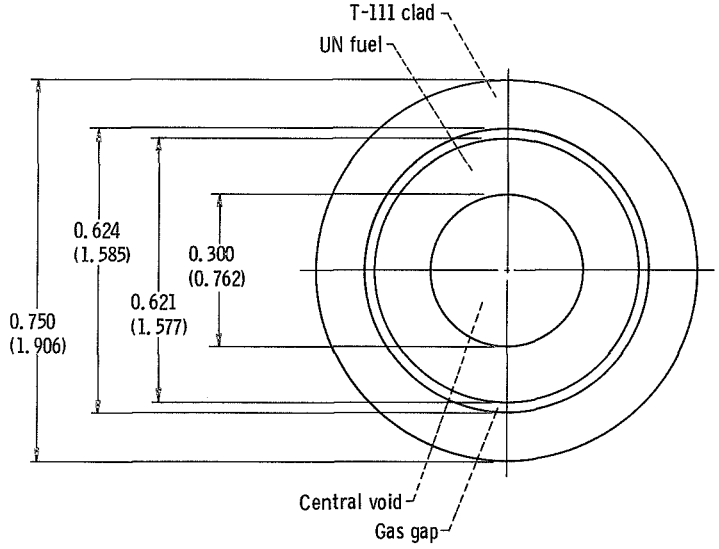

Figure 4. - Fuel-pin geometry. (Dimensions are in inches (cm).)

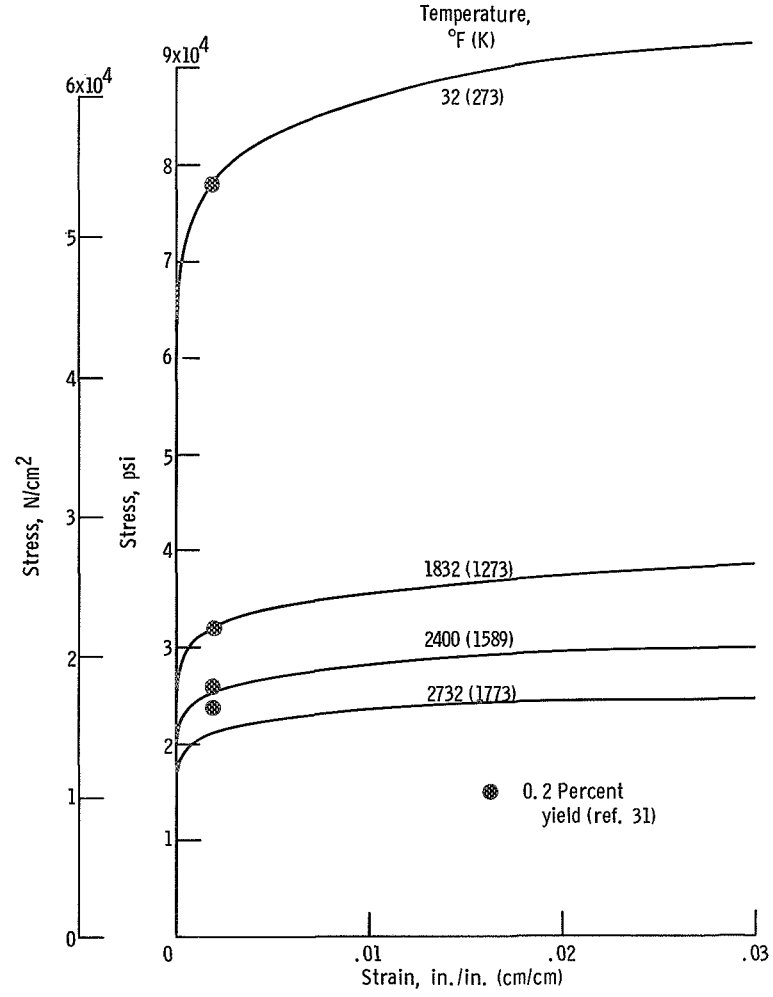

Figure 5. - Stress-strain diagram for T-111 alloy.

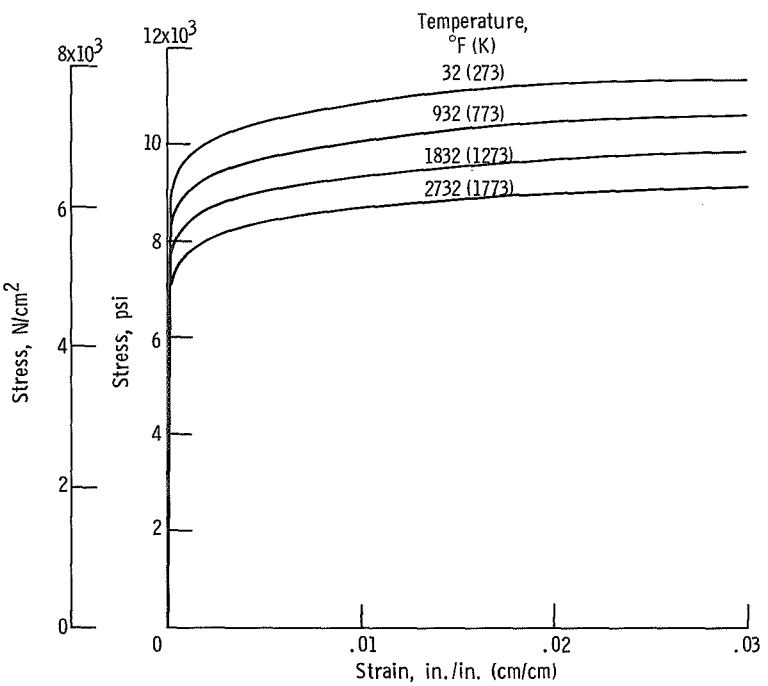

Figure 6. - Stress-strain diagram for uranium nitride.

NATIONAL AERONAUTICS AND SPACE ADMINISTRATION
WASHINGTON, D.C. 20546

OFFICIAL BUSINESS
PENALTY FOR PRIVATE USE $300

FIRST CLASS MAIL

POSTAGE AND FEES PAID
NATIONAL AERONAUTICS AND
SPACE ADMINISTRATION

POSTMASTER: If Undeliverable (Section 158
Postal Manual) Do Not Return

"The aeronautical and space activities of the United States shall be conducted so as to contribute . . . to the expansion of human knowledge of phenomena in the atmosphere and space. The Administration shall provide for the widest practicable and appropriate dissemination of information concerning its activities and the results thereof."

—NATIONAL AERONAUTICS AND SPACE ACT OF 1958

NASA SCIENTIFIC AND TECHNICAL PUBLICATIONS

TECHNICAL REPORTS: Scientific and technical information considered important, complete, and a lasting contribution to existing knowledge.

TECHNICAL NOTES: Information less broad in scope but nevertheless of importance as a contribution to existing knowledge.

TECHNICAL MEMORANDUMS: Information receiving limited distribution because of preliminary data, security classification, or other reasons.

CONTRACTOR REPORTS: Scientific and technical information generated under a NASA contract or grant and considered an important contribution to existing knowledge.

TECHNICAL TRANSLATIONS: Information published in a foreign language considered to merit NASA distribution in English.

SPECIAL PUBLICATIONS: Information derived from or of value to NASA activities. Publications include conference proceedings, monographs, data compilations, handbooks, sourcebooks, and special bibliographies.

TECHNOLOGY UTILIZATION PUBLICATIONS: Information on technology used by NASA that may be of particular interest in commercial and other non-aerospace applications. Publications include Tech Briefs, Technology Utilization Reports and Technology Surveys.

Details on the availability of these publications may be obtained from:

SCIENTIFIC AND TECHNICAL INFORMATION OFFICE

NATIONAL AERONAUTICS AND SPACE ADMINISTRATION

Washington, D.C. 20546